### **Mathematical Biology**



# Predator-induced prey dispersal can cause hump-shaped density-area relationships in prey populations

James T. Cronin<sup>1</sup> · Jerome Goddard II<sup>2</sup> · Amila Muthunayake<sup>3</sup> · Juan Quiroa<sup>4</sup> · Ratnasingham Shivaji<sup>5</sup>

Received: 19 January 2023 / Revised: 29 September 2023 / Accepted: 28 November 2023 © The Author(s), under exclusive licence to Springer-Verlag GmbH Germany, part of Springer Nature 2024

### Abstract

Predation can both reduce prey abundance directly (through density-dependent effects) and indirectly through prey trait-mediated effects. Over the years, many studies have focused on describing the density-area relationship (DAR). However, the mechanisms responsible for the DAR are not well understood. Loss and fragmentation of habitats, owing to human activities, creates landscape-level spatial heterogeneity wherein patches of varying size, isolation and quality are separated by a human-modified "matrix" of varying degrees of hostility and has been a primary driver of species extinctions and declining biodiversity. How matrix hostility in combination with trait-mediated effects influence DAR, minimum patch size, and species coexistence remains

James T. Cronin, Jerome Goddard II, Amila Muthunayake, Juan Quiroa and Ratnasingham Shivaji are contributed equally to this work.

☑ Jerome Goddard II igoddard@aum.edu

James T. Cronin jcronin@lsu.edu

Amila Muthunayake amilamuthunayake@weber.edu

Juan Quiroa jequiroa@ncsu.edu

Ratnasingham Shivaji r\_shivaj@uncg.edu

Published online: 25 January 2024

- Department of Biological Sciences, Louisiana State University, Baton Rouge, LA 70803, USA
- Department of Mathematics, Auburn University Montgomery, Montgomery, AL 36124, USA
- Department of Mathematics, Weber State University, Ogden, UT 84408, USA
- Department of Mathematics, North Carolina State University, Raleigh, NC 27607, USA
- Department of Mathematics and Statistics, University of North Carolina Greensboro, NC 27412, USA



20 Page 2 of 31 J. T. Cronin et al.

an open question. In this paper, we employ a theoretical spatially explicit predator-prey population model built upon the reaction-diffusion framework to explore effects of predator-induced emigration (trait-mediated emigration) and matrix hostility on DAR, minimum patch size, and species coexistence. Our results show that when trait-mediated response strength is sufficiently strong, ranges of patch size emerge where a nonlinear hump-shaped prey DAR is predicted and other ranges where coexistence is not possible. In a conservation perspective, DAR is crucial not only in deciding whether we should have one large habitat patch or several-small (SLOSS), but for understanding the minimum patch size that can support a viable population. Our study lends more credence to the possibility that predators can alter prey DAR through predator-induced prey dispersal.

**Keywords** Predator-induced emigration · Trait-mediated emigration · Density-area relationship · Reaction diffusion model · Ecological release · Dispersal release

**Mathematics Subject Classification** 92D40 · 35J25

### 1 Introduction

### 1.1 Background and motivation

Predators have both direct (density-mediated) and indirect (trait-mediated indirect) effects on prey populations (Werner and Peacor 2003; Cronin et al. 2004; Holt and Barfield 2012; Ohgushi et al. 2012). As an example, most predator–prey studies are concerned with the rate of prey consumption by a predator and those effects on prey density (a density-mediated effect), as opposed to predator influence on the phenotype of the surviving prey (a trait-mediated indirect effect; see Werner and Peacor 2003; Ohgushi et al. 2012; Irwin 2012). In fact, it is now generally accepted that ecological communities are replete with trait-mediated indirect effects arising from phenotypic plasticity and these effects are important to community dynamics (Schmitz 2003; Werner and Peacor 2003; Holt and Barfield 2012). These trait-mediated indirect effects are also expected to contribute strongly to many phenomena that traditionally have been solely attributed to density-mediated effects (Werner and Peacor 2003; Holt and Barfield 2012; Ohgushi et al. 2012).

Trait-mediated behavioral responses to predators can affect the dynamics of a population significantly (see Werner and Peacor 2003; Holt and Barfield 2012; Ohgushi et al. 2012). One such effect is trait-mediated dispersal, in which the prey changes its dispersal patterns due to the presence of a predator, which can, in turn, modify population dynamics and species interactions (see Cantrell and Cosner 2018, for example). This idea has been considered in empirical studies in the predator–prey context (though scarcely), where increased predation risk was shown to increase emigration rates of prey. For example, Cronin et al. (2004) found evidence of predator-induced emigration in a spider (predator) and planthopper (prey) system, and even concluded that at high predator density, the predator had a greater impact on prey density through induced emigration than consumption (also see Sih et al. 1992; Hakkarainen et al. 2001; Peckarsky 1996).



The loss and fragmentation of habitats due to anthropogenic activities has been a growing problem over the past several centuries (e.g., Heilman et al. 2002; Ewers et al. 2013; Uchida and Ushimaru 2014). This fragmentation creates landscape-level spatial heterogeneity wherein patches of varying size, isolation and quality are separated by a human-modified "matrix" of varying degrees of hostility. Studies of trait-mediated predator effects at the landscape scale have focused on quantifying the spatial variation in predation risk (i.e., the "landscape of fear", sensu Laundré et al. 2001) and habitat use by prey (e.g., Matassa and Trussell 2011; Laundré et al. 2014; Sand et al. 2021). However, to our knowledge, trait-mediated indirect effects of predators on prey populations, and their consequences for density-area relationships (DARs), minimum patch size, and species coexistence have not been addressed in the context of this landscape heterogeneity.

Matrix composition or hostility is an important component of a landscape and can have profound effects on species movement and boundary behavior, persistence of a single species (e.g., Haynes and Cronin 2003; Fonseka et al. 2020a; Goddard et al. 2019; Cronin et al. 2019a, b) and coexistence of interacting species (e.g. a host-parasitoid system in Cronin (2007) and a competitive system in Cantrell et al. (1998) and Cantrell et al. (2004)). In fact, matrix quality degradation has been shown to cause a reversal in competitive dominance in a theoretical model of two competitive species (see Cantrell et al. 1998, 2004; Acharya et al. 2023). How matrix hostility in combination with trait-mediated effects influence DAR, minimum patch size, and species coexistence remains an open question.

Over the years, many studies have focused on describing the density-area relationship (Bender et al. 1998; Bowers and Matter 1997; Connor et al. 2000; Hambäck and Englund 2005). However, the mechanisms responsible for the DAR are not well understood (Jackson et al. 2013). A better understanding of mechanistic causes of DARs underpins basic ecological theory and is important for development of appropriate conservation plans and improving species-area distribution predictions (Jackson et al. 2013; Matter 1999). In most metapopulation models, an implicit assumption is made that density does not vary with patch size, i.e. a neutral DAR (Hanski 1999). However, non-neutral DAR result in animals clustering in small, intermediate, or large patches, which in turn changes the relative importance of different size patches. This change could potentially alter metapopulation predictions of persistence (Matter 1999). From a conservation perspective, the relationship between reserve size and population density is central to the single large or several-small (SLOSS) debate (Simberloff and Abele 1982; Matter 1999; Bowers and Matter 1997; Heilman et al. 2002; Lindenmayer et al. 2015; Mccarthy et al. 2005). The density-area relationship is also intrinsically linked to the species-area relationship (SAR) (see e.g., Matter 2000; Buckley and Roughgarden 2006). In fact, the literature addressing DAR is relatively small compared to addressing SAR (Buckley and Roughgarden 2006).

The simplest a priori expectation is that, for habitat specialists, restricted to habitat fragments or patches, population density should increase with patch area, i.e. a positive DAR (Debinski and Holt 2000). Several meta-analysis studies have been done to generalize DAR, but have found inconsistent results across taxa and experiments. To move beyond correlative analyses and search for underlying mechanisms, a deeper understanding of DAR is needed (Hambäck and Englund 2005). Notwithstanding, sev-



eral studies provide evidence for nonlinear DARs and link them to ecological release (i.e., the density-compensation hypothesis; MacArthur 1972). For example, Buckley and Roughgarden (2006) observed a hump-shaped DAR in Anolis lizards inhabiting the Grenadines islands—islands with area below a certain threshold showed a positive DAR, whereas islands with area above this threshold exhibited a negative DAR. They found that habitat diversity exhibited a positive relationship with insular area and suggested that increasing avian predation or competition with habitat diversity can account for this nonlinear DAR. Wright (1981) and Wright et al. (1984) found essentially the same result for Anolis lizards inhabiting the West Indies Islands. Goddard et al. (2023) modeled DAR via a Lotka-Volterra reaction diffusion model with absorbing boundary conditions in scenarios that qualitatively matched these empirical studies. It was shown that competitive release as patch size decreased to one of the competitor's minimum patch size generated model predictions of an overall hump-shaped DAR which is qualitatively similar to those observed in nature.

In this paper, we propose that trait-mediated dispersal via predator-induced emigration (PIE) (or, simply, trait-mediated emigration) can have profound effects on DAR, minimum patch size, and species coexistence, ultimately causing an overall hump-shaped DAR to arise in prey. Moreover, we propose that matrix hostility will also play an integral role. We employ a theoretical spatially explicit population model built upon the reaction diffusion framework to test these predictions.

### 1.2 Model formulation

We propose a model designed to explore effects of trait-mediated emigration similar to what was observed in the empirical study of Cronin et al. (2004). Suppose that a predator-prey system inhabits a single focal patch  $\Omega_0 = \{\ell x \mid x \in \Omega\}$ . Here, patch size is represented by  $\ell > 0$ ,  $\Omega = (0, 1)$  or  $\Omega \subset \mathbb{R}^n$  having unit measure (e.g. if n = 2then the area of  $\Omega$  is one) and smooth boundary with n=2,3. The patch is surrounded by a hostile matrix, denoted by  $\Omega_M = \mathbb{R}^n \backslash \overline{\Omega}_0$ , with an assumption that organisms experience exponential decay at fixed rate (say,  $S_0 > 0$ ). Denote the boundary of  $\Omega_0$ by  $\partial \Omega_0$ , u(t, x) as the predator's density, and v(t, x) as the prey's density for time t and spatial location x within the patch. In order to disentangle direct (consumptive) from indirect (trait-mediated) effects, we assume that the predator is a generalist with consumptive effect on this prey being negligible. This approach closely follows that of empirical studies which have used an analogous approach to partition density- from trait-mediated effects; for example, Oswald (1998) glued the mouthparts of spiders together to prevent them from consuming prey while allowing them to affect prey dispersal. Our main goal here is to show the varied consequences of trait-mediated emigration on system dynamics. Thus, both species obey logistic growth laws, the predator exhibits density-independent emigration (DIE), and prey exhibit intraspecific DIE and trait-mediated emigration via a positive relationship between predator density and emigration (+DDE). In this way, an increase in the predator density will cause an increase in prey emigration rate, which in turn will cause higher mortality for prey as they move back and forth between the patch and hostile matrix.



An unbiased random walk is assumed inside patch and matrix with a biased random walk on the patch/matrix interface. Discontinuity between the density in the patch and matrix is allowed at the interface and continuity in the flux is maintained (see e.g. Maciel et al. 2013; Ovaskainen and Cornell 2003; Ovaskainen 2004). Both species recognize the patch/matrix interface and modify their random walk movement probability (i.e., probability of an organism moving at a given time step in the random walk process), random walk step length (i.e., distance that an organism moves during a given time step), and probability of remaining in the patch (say  $\alpha_i$ ). Patch dispersal is equivalent to organisms reaching the patch/matrix interface, leaving the patch with probability  $1 - \alpha_i$ , and entering the matrix. Note that they still have the opportunity to re-enter the patch from the matrix at the interface. Following the derivation given in Cronin et al. (2019a), a model describing this situation is:

$$\begin{cases} u_{t} = D_{1}\Delta u + r_{1}u(1-u); & t > 0, x \in \Omega_{0} \\ v_{t} = D_{2}\Delta v + r_{2}v(1-v); & t > 0, x \in \Omega_{0} \\ u(0, x) = u_{0}(x); & x \in \Omega_{0} \\ v(0, x) = v_{0}(x); & x \in \Omega_{0} \\ D_{1}\alpha_{1}\frac{\partial u}{\partial \eta} + S_{1}^{*} [1-\alpha_{1}]u = 0; & t > 0, x \in \partial\Omega_{0} \\ D_{2}\alpha_{2}(u)\frac{\partial v}{\partial \eta} + S_{2}^{*} [1-\alpha_{2}(u)]v = 0; & t > 0, x \in \partial\Omega_{0}. \end{cases}$$

$$(1)$$

We remark that (1) will exactly model the study system for a one-dimensional patch in the sense that steady states of (1) and their stability properties will be exactly the same as those of the study system (see Appendix C of Cronin et al. 2019a and references therein), while providing a reasonable approximation of the study system for a simply connected, convex patch in two- or three-dimensions. Here,  $D_i > 0$  denotes patch diffusion rate,  $r_i > 0$  patch intrinsic growth rate,  $u_0(x)$ ,  $v_0(x)$  initial population density distributions in the patch,  $\alpha_i$  the probability of an individual remaining in the patch upon reaching the boundary (i = 1 for u and i = 2 for v), and carrying capacities have been normalized to one. The outward normal derivative operator is denoted by  $\frac{\partial}{\partial n}$ . From the derivation in Cronin et al. (2019a),  $S_i^* \geq 0$  is the effective matrix hostility, has units of length by time, and can assume different forms depending upon the patch/matrix interface assumptions. A given relationship between density and emigration can now be included in the model by selecting appropriate  $\alpha_i$ 's (see, for example, Cantrell and Cosner 2007, 2006; Cronin et al. 2019a, 2020, 2019b; Harman et al. 2020; Fonseka et al. 2020b; Goddard et al. 2019). Here, we choose  $\alpha_1 \equiv \frac{1}{2}$  and  $\alpha_2(u) = \frac{M}{2M+u}$  where M > 0 is a parameter with units of density. Notice that in absence of predators, prey emigration rate is 50%.

Non-dimensionalization of both parameters and variables by "scales" or units allows mathematical representation of analogous biological scenarios using a simplified model with fewer parameters. Although several rescalings are possible, we follow Cronin et al. (2019a) and choose,

$$\tilde{x} = \frac{x}{\ell} \& \tilde{t} = r_1 t. \tag{2}$$



20 Page 6 of 31 J. T. Cronin et al.

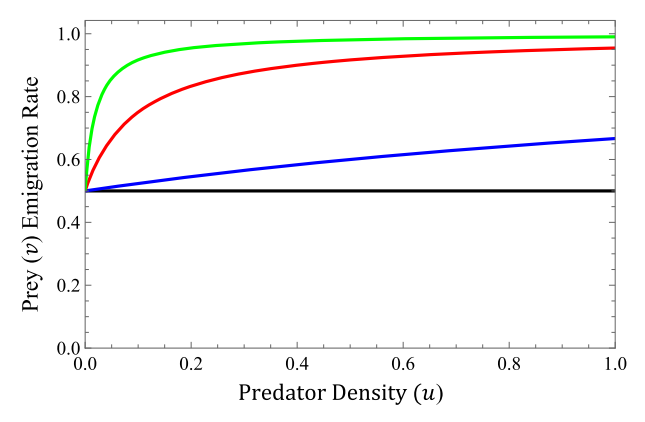


**Fig. 1** Plot of predator density (*u*) versus prey (*v*) emigration rate for various trait-mediated effect strengths:  $\beta = 0$  (black),  $\beta = 1$  (blue),  $\beta = 20$  (red),  $\beta = 100$  (green)

Applying this scaling and dropping the tilde, (1) becomes

$$\begin{cases} u_{t} = \frac{1}{\lambda} \Delta u + u(1-u); & t > 0, x \in \Omega \\ v_{t} = \frac{D_{0}}{\lambda} \Delta v + r_{0}v(1-v); & t > 0, x \in \Omega \\ u(0, x) = u_{0}(x); & x \in \Omega \\ v(0, x) = v_{0}(x); & x \in \Omega \\ \frac{\partial u}{\partial \eta} + \sqrt{\lambda} \gamma_{1} u = 0; & t > 0, x \in \partial \Omega \\ \frac{\partial v}{\partial \eta} + \sqrt{\lambda} \gamma_{2} g(u) v = 0; & t > 0, x \in \partial \Omega \end{cases}$$

$$(3)$$

with corresponding steady state equations:

$$\begin{cases} -\Delta u = \lambda u(1-u); \ \Omega \\ \frac{\partial u}{\partial \eta} + \sqrt{\lambda} \gamma_1 u = 0; \ \partial \Omega \end{cases}$$
 (4)

and

$$\begin{cases}
-\Delta v = \lambda r v (1 - v); \ \Omega \\
\frac{\partial v}{\partial \eta} + \sqrt{\lambda} \gamma_2 g(u) v = 0; \ \partial \Omega
\end{cases}$$
(5)

where  $\lambda = \frac{r_1\ell^2}{D_1}$ ,  $r_0 = \frac{r_2}{r_1}$ ,  $D_0 = \frac{D_2}{D_1}$ ,  $r = \frac{r_0}{D_0}$ ,  $\gamma_1 = \frac{S_1^*}{\sqrt{r_1D_1}} \frac{1-\alpha_1}{\alpha_1}$ ,  $\gamma_2 = \frac{S_2^*}{\sqrt{r_1D_1D_0}}$ , and  $g(u) = \beta u + 1$  (here,  $\beta = \frac{1}{M}$ ) are all unitless. We note that  $\beta$  measures trait-mediated effect strength. In particular, prey emigration rate is constant for  $\beta = 0$ , increases slowly with respect to predator density and to a maximum well below 100% for small  $\beta$ -values, and increases to near 100% for even small predator densities for large  $\beta$ -values. Figure 1 shows predator density (u) versus prey (v) emigration rate for several  $\beta$ -values. Also, recall that  $\Omega$  has length, area, or volume of one. For fixed  $r_1, r_2, D_1, D_2$ , the composite parameter  $\lambda$  is proportional to patch size squared,  $\gamma_1$  represents combined matrix hostility towards v.



Notice that r can be written as  $r = \frac{\frac{r_2}{D_2}}{\frac{r_1}{D_1}}$  and interpreted as a means to compare the two species by their growth-to-diffusion (G-D) ratio, defined as the ratio of patch intrinsic growth rate to patch diffusion rate. There are three cases for r: (1) if r = 1, then both G-D ratios are the same, (2) if r > 1 then v's G-D ratio is greater than u's, and (3) if r < 1 then u's G-D ratio is greater than v's.

### 1.3 Structure of the paper

We will present some preliminary mathematical results in Sect. 2. In Sect. 3, we state and prove our main results, followed by discussion of their implications. Finally, we give concluding remarks in Sect. 4.

### 2 Mathematical preliminaries

In this section, we provide two main mathematical tools which we will employ to analyze the model (3). The first tool is a theorem providing complete dynamics of single species model where emigration from the patch is assumed to be a generic function of patch size via the composite parameter,  $\lambda$ , namely:

$$\begin{cases} w_t = \frac{1}{\lambda} \Delta w + f(w); & t > 0, x \in \Omega \\ w(0, x) = w_0(x); & x \in \Omega \\ \frac{\partial w}{\partial \eta} + \mu(\lambda)(x)w = 0; & t > 0, x \in \partial \Omega \end{cases}$$
 (6)

with steady state equation

$$\begin{cases} -\Delta w = \lambda f(w); & \Omega \\ \frac{\partial w}{\partial \eta} + \mu(\lambda)(x)w = 0; & \partial \Omega \end{cases}$$
 (7)

where  $\lambda > 0$ ,  $w_0: \Omega \to [0, \infty)$  is a smooth function, f is a function that exhibits logistic-type growth behavior in satisfying

**(H1):**  $f:[0,\infty)\to\mathbb{R}$  is a smooth function with

- (a) f(0) = 0 and f'(0) > 0
- (b) There is a K > 0 such that: f(u) > 0; (0, K), f(K) = 0, f(u) < 0;  $(K, \infty)$
- (c) f''(s) < 0 for  $s \in [0, K]$

and  $\mu(\lambda): \partial\Omega \to [0, \infty)$  is a smooth function for all  $\lambda \in [0, \infty)$ . For convenience of presentation, we assume that K=1. However, this assumption will not cause a qualitative change in our analysis. In what follows, we will show that the complete dynamics of (6) can be determined via study of stability properties of the trivial solution of (7). This, in turn can be determined via sign of the principal eigenvalue  $\sigma(\lambda, \mu(\lambda))$  of

$$\begin{cases} -\Delta \phi - \lambda f'(0)\phi = \sigma \phi; \ \Omega \\ \frac{\partial \phi}{\partial \eta} + \mu(\lambda)(x)\phi = 0; \ \partial \Omega \end{cases}$$
 (8)

20 Page 8 of 31 J. T. Cronin et al.

with corresponding eigenfunction  $\phi$  which can be chosen such that  $\phi > 0$ ;  $\overline{\Omega}$ . Notice that (8) is the linearization of (7) about the trivial solution. We also recall the classical Robin boundary eigenvalue problem,

$$\begin{cases}
-\Delta \widetilde{\phi} = \widetilde{E} R \widetilde{\phi}; \ \Omega \\
\frac{\partial \widetilde{\phi}}{\partial \eta} + b(x) \widetilde{\phi} = 0; \ \partial \Omega.
\end{cases}$$
(9)

For fixed R>0 and  $b(x)\geq 0$ ;  $\partial\Omega$ , it is well known that (9) has a principal eigenvalue, which we will denote as  $\widetilde{E}_1(R,b)$ , with corresponding eigenfunction  $\widetilde{\phi}$  that can be chosen such that  $\widetilde{\phi}>0$ ;  $\overline{\Omega}$  (see Cantrell and Cosner 2003, for example). We will also denote  $\widetilde{E}_1^D(R)>0$  as the principal eigenvalue of (9) with Dirichlet boundary condition and recall that for fixed R>0, we have that 1)  $\widetilde{E}_1(R,0)=0$ , 2)  $\widetilde{E}_1(R,b)$  is increasing in b in the sense that if  $b_1(x)< b_2(x)$ ;  $\partial\Omega$  then  $\widetilde{E}_1(R,b_1)< \widetilde{E}_1(R,b_2)$ , and 3)  $\widetilde{E}_1(R,b)\to \left(\widetilde{E}_1^D(R)\right)^-$  when  $b(x)=b_0$  is constant and  $b_0\to\infty$ . (see Cantrell and Cosner 2003). In the special case that  $b(x)\equiv\sqrt{\lambda}\gamma$  and  $\gamma\geq0$ , we will write  $E_1(R,\gamma)=\widetilde{E}_1(R,\sqrt{\lambda}\gamma)$ . Also, we recall the property

$$E_1(R,\gamma) = \frac{E_1(1,\frac{\gamma}{\sqrt{R}})}{R} \tag{10}$$

as proved in Cronin et al. (2020), denote  $E_1^D = \widetilde{E}_1^D(1)$  and with  $\widetilde{E}_1^D(R) = \frac{E_D^1}{R}$ , and recall part (D) of Lemma 2.7 from Acharya et al. (2023):

**Lemma 1** Fix  $\gamma_1 > 0$  and  $\gamma_2 \ge 0$  then there exists an unique  $r^*(\gamma_1, \gamma_2) > 0$  such that,

- (i) if  $r < r^*(\gamma_1, \gamma_2)$  then  $E_1(1, \gamma_1) < E_1(r, \gamma_2)$
- (ii) if  $r = r^*(\gamma_1, \gamma_2)$  then  $E_1(1, \gamma_1) = E_1(r, \gamma_2)$
- (iii) if  $r > r^*(\gamma_1, \gamma_2)$  then  $E_1(1, \gamma_1) > E_1(r, \gamma_2)$
- (iv) if  $\gamma_1 > \gamma_2$  then  $r^*(\gamma_1, \gamma_2) < 1$
- (v) if  $\gamma_1 = \gamma_2$  then  $r^*(\gamma_1, \gamma_2) = 1$
- (vi) if  $\gamma_1 < \gamma_2$  then  $r^*(\gamma_1, \gamma_2) > 1$ .

Lemma 1 provides a connection between G-D ratio  $(r = \frac{\frac{r_1}{D_2}}{\frac{r_1}{D_1}})$  and combined matrix hostility  $(\gamma_1 \& \gamma_2)$  and minimum patch size of the species in the absence of the other. To see this, we recall our definition of  $\lambda = \frac{r_1\ell^2}{D_1}$  giving predator minimum patch size as  $\ell_1^* = \sqrt{\frac{E_1(1,\gamma_1)D_1}{r_1}}$  and prey in the absence of predators as  $\ell_2^* = \sqrt{\frac{E_1(r,\gamma_2)D_1}{r_1}}$  (see Cronin et al. 2019a). Here, we consider stability in the Lyapunov sense (e.g., see Pao 1992) and state a lemma from Goddard II and Shivaji (2017) which provides a connection between stability of the trivial solution of (7) and sign of the principal eigenvalue  $\overline{\sigma}(\lambda, \mu(\lambda))$  of the eigenvalue problem:

$$\begin{cases} -\Delta \overline{\phi} - \lambda f'(0)\overline{\phi} = \overline{\sigma}\overline{\phi}; \ \Omega \\ \frac{\partial \overline{\phi}}{\partial \eta} + \mu(\lambda)(x)\overline{\phi} = \overline{\sigma}\overline{\phi}; \ \partial \Omega \end{cases}$$
 (11)



with corresponding eigenfunction  $\overline{\phi}$  which can be chosen such that  $\overline{\phi} > 0$ ;  $\overline{\Omega}$  (see Amann 1976 for existence of such a principal eigenvalue).

**Lemma 2** (Goddard II and Shivaji (2017)) *Let*  $\overline{\sigma}(\lambda, \mu(\lambda))$  *be the principal eigenvalue of* (11). *Then the following hold:* 

- (A) If  $\overline{\sigma}(\lambda, \mu(\lambda)) \geq 0$  then the trivial solution of (7) is stable. Furthermore, if the trivial solution is isolated from other solutions of (7) then the trivial solution is asymptotically stable.
- (B) If  $\overline{\sigma}(\lambda, \mu(\lambda)) < 0$  then the trivial solution of (7) is unstable.

Note that the argument given in Lemma 5 of Appendix 2 in Goddard et al. (2018) goes through here yielding  $sgn(\sigma(\lambda, \mu(\lambda))) = sgn(\overline{\sigma}(\lambda, \mu(\lambda)))$ . Thus, it suffices to only consider the sign of  $\sigma(\lambda, \mu(\lambda))$ .

We can now extend the results in Goddard et al. (2018) to the case of (6) and prove:

**Theorem 3** Suppose that (H1) holds and  $\mu(\lambda)$  is a smooth nonnegative function. Then we have the following:

- (A) If  $\sigma(\lambda, \mu(\lambda)) \ge 0$  then  $w \equiv 0$  is globally asymptotically stable and no positive solution exists for (7).
- (B) If  $\sigma(\lambda, \mu(\lambda)) < 0$  then  $w \equiv 0$  is unstable and there exists a unique globally asymptotically stable positive solution  $w(\lambda, \mu(\lambda))$  for (7). Moreover, the following properties of  $w(\lambda, \mu(\lambda))$  hold:
  - (i)  $w(\lambda, \mu(\lambda)) < 1$ ;  $x \in \overline{\Omega}$
  - (ii) Let  $\lambda_1$  be a solution of  $\widetilde{E}_1(f'(0), \mu(\lambda)) = \lambda$ . Then if  $\sigma(\lambda, \mu(\lambda)) \to 0^-$  as  $\lambda \to \lambda_1^+, (\lambda \to \lambda_1^-)$ , then  $w(\lambda, \mu(\lambda)) \to 0^+$  on  $\Omega$  as  $\lambda \to \lambda_1^+, (\lambda \to \lambda_1^-)$ .
  - (iii) If  $\sigma(\lambda, \mu(\lambda)) < 0$  for all  $\lambda > \lambda_2$  (for some  $\lambda_2 > 0$ ), then  $w(\lambda, \mu(\lambda)) \to 1^-$  uniformly on every closed subset of  $\Omega$  as  $\lambda \to \infty$ .
  - (iv)  $w(\lambda, \mu(\lambda))$  is a decreasing function of  $\mu$ , in the following sense: if  $\mu_1(\lambda)(x) \le \mu_2(\lambda)(x)$  then  $w(\lambda, \mu_1(\lambda)(x)) \ge w(\lambda, \mu_2(\lambda)(x))$ ;  $x \in \overline{\Omega}$ .
  - (v) Let  $\lambda^* > \lambda^{**}$  and  $\mu(\lambda^*)(x) \leq \mu(\lambda^{**})(x)$ ;  $x \in \overline{\Omega}$ . Then  $w(\lambda^*, \mu(\lambda^*))(x) \geq w(\lambda^{**}, \mu(\lambda^{**}))(x)$ ;  $x \in \overline{\Omega}$ .

A proof of Theorem 3 is provided in Sect. 2.1.

Thus, the sign of  $\sigma(\lambda, \mu(\lambda))$  and Theorem 3 give complete dynamics of (3) by making appropriate choices of  $\mu(\lambda)$  and f(w), noting that  $f_1(u) = u(1-u)$  and  $f_2(v) = rv(1-v)$  both satisfy (H1) with  $f'_1(0) = 1$  and  $f'_2(0) = r$ , respectively.

In particular, for fixed  $\lambda > 0$ , if f(w) = w(1 - w) and  $\mu_1(\lambda)(x) = \sqrt{\lambda}\gamma_1$ ;  $x \in \partial \Omega$  then the unique positive solution of (4) is given by  $u(\lambda) \equiv w(\lambda, \mu_1(\lambda))$  (see Goddard et al. 2018 for details). In this case, comparing (8) with (9) and using the fact that principal eigenvalues are unique, we have the following characterization of  $\sigma(\lambda, \mu_1(\lambda))$ :

$$\sigma(\lambda, \mu_1(\lambda)) = \widetilde{E}_1\left(1, \sqrt{\lambda}\gamma_1\right) - \lambda, \tag{12}$$

which when  $\sigma(\lambda, \mu_1(\lambda)) = 0$  has the unique solution  $\lambda = E_1(1, \gamma_1) = \widetilde{E}_1(1, \sqrt{\lambda}\gamma_1)$  (again, see Goddard et al. 2018 for details). Thus, we must also have:

$$\sigma(\lambda, \mu_1(\lambda)) \geq 0$$
 if and only if  $\lambda \leq E_1(1, \gamma_1)$ 

20 Page 10 of 31 J. T. Cronin et al.

$$\sigma(\lambda, \mu_1(\lambda)) < 0 \text{ if and only if } \lambda > E_1(1, \gamma_1).$$
 (13)

If for fixed  $\lambda > 0$  we have  $u(\lambda) \equiv 0$ , f(w) = rw(1-w), and  $\mu(\lambda)(x) = \mu_2(\lambda)(x) = \sqrt{\lambda}\gamma_2$ ;  $x \in \partial\Omega$  (using the fact that g(0) = 1) then the unique positive solution of (5) is  $v(\lambda) \equiv w(\lambda, \mu_2(\lambda))$ . Again, comparing (8) with (9) and using the fact that principal eigenvalues are unique, we have the following characterization of  $\sigma(\lambda, \mu_2(\lambda))$ :

$$\sigma(\lambda, \mu_2(\lambda)) = r\widetilde{E}_1\left(r, \sqrt{\lambda}\gamma_2\right) - \lambda r,\tag{14}$$

which when  $\sigma(\lambda, \mu_2(\lambda)) = 0$  has the unique solution  $\lambda = E_1(r, \gamma_2) = \widetilde{E}_1(r, \sqrt{\lambda}\gamma_2)$ . Thus, we must also have:

$$\sigma(\lambda, \mu_2(\lambda)) \ge 0$$
 if and only if  $\lambda \le E_1(r, \gamma_2)$   
 $\sigma(\lambda, \mu_2(\lambda)) < 0$  if and only if  $\lambda > E_1(r, \gamma_2)$ . (15)

In the case when  $\lambda > E_1(1, \gamma_1)$  implying that  $u(\lambda)$  exists,  $v(\lambda)$  is found in a similar manner, i.e., using this  $u(\lambda)$  with f(w) = rw(1 - w) and  $\mu_3(\lambda)(x) = \sqrt{\lambda}\gamma_2(\beta u(\lambda)(x) + 1)$  we have that the unique positive solution of (5) is  $v(\lambda) \equiv w(\lambda, \mu_3(\lambda))$ . A characterization of  $\sigma(\lambda, \mu_3(\lambda))$  is much more delicate, and we will postpone that discussion until Sect. 3.

Also, let  $\sigma_0(\lambda)$  be the principal eigenvalue of

$$\begin{cases} -\Delta\phi_0 - \lambda r\phi_0 = \sigma_0\phi_0; \ \Omega\\ \phi_0 = 0; \ \partial\Omega \end{cases}$$
 (16)

with corresponding eigenfunction  $\phi_0 > 0$ ;  $\Omega$  with  $\|\phi_0\| = 1$ . We now state a Lemma that gives comparisons between  $\sigma(\lambda, \mu_2(\lambda))$ ,  $\sigma(\lambda, \mu_3(\lambda))$ , and  $\sigma_0(\lambda)$ . Its proof is given in Sect. 2.2.

**Lemma 4** For fixed  $\gamma_1, \gamma_2, r > 0$  and  $\beta \geq 0$  we have that  $\sigma(\lambda, \mu_2(\lambda)) \leq \sigma(\lambda, \mu_3(\lambda)) < \sigma_0(\lambda)$  for all  $\lambda > E_1(1, \gamma_1)$ .

Secondly, we recall a method to study the structure of positive steady states of (3) in the special case of  $\Omega=(0,1)$  and  $\mu(\lambda)(0)=\mu(\lambda)(1)$ . This method given in Theorem 5 is referred to as a time map analysis (or quadrature method) and is proved in Cronin et al. (2019b). Note that in this case, Lemma 5.1 in Cronin et al. (2019b) ensures symmetry of  $w(\lambda,\mu(\lambda))$  about  $x=\frac{1}{2}$  implying that  $w(\lambda,\mu(\lambda)(0)=w(\lambda,\mu(\lambda)(1))$ .

**Theorem 5** (Cronin et al. (2019b)) A positive solution,  $w(\lambda, \mu(\lambda))$ , of (7) with  $\rho = \|w(\lambda, \mu(\lambda))\|_{\infty}$ ,  $q = w(\lambda, \mu(\lambda))(0) = w(\lambda, \mu(\lambda))(1)$  exists if and only if  $\lambda > 0$ ,  $\rho \in (0, 1)$ , and  $q \in [0, \rho)$  satisfy:

$$\lambda = 2\left(\int_{q}^{\rho} \frac{ds}{\sqrt{F(\rho) - F(s)}}\right)^{2} \tag{17}$$

and

$$2\lambda [F(\rho) - F(q)] = [\mu(\lambda)(0)]^2 q^2$$
 (18)



where  $F(s) = \int_0^s f(t)dt$ .

**Remark 1** For  $\rho \in (0, 1)$ , since  $f(\rho) > 0$ , it can be shown that the improper integral in (17) is convergent.

We employ the following procedure to produce bifurcation diagrams of positive solutions for (4)–(5) via Theorem 5. Fixing r,  $\gamma_1$ ,  $\gamma_2 > 0$ , and  $\beta \geq 0$ , we let  $\rho_i = \frac{i}{n+1}$ ; i=1,...,n for some  $n\geq 1$ . Setting  $\rho=\rho_1$ , we solve equation (18) for q using the FindRoot command in Mathematica (Wolfram Inc., ver. 13.1). The values of q and  $\rho$  are then substituted into (17) to find the corresponding value of  $\lambda$ . We then employ a shooting method via NDSolve to numerically approximate the solution, u or v. To calculate average density, we then employ NIntegrate to approximate  $d=\int_0^1 w(\lambda,\mu(\lambda))(x)dx$  (recall that  $\|\Omega\|=1$ ) where w=u or w=v. Repeating this procedure for  $\rho=\rho_i, i=2,...,n$ , we obtain  $(\lambda,d)$  points generating a bifurcation diagram of  $\lambda$  vs. d (average density) for positive solutions of (4)–(5).

### 2.1 Proof of Theorem 3

Suppose that (H1) holds and  $\mu(\lambda)$  is a smooth nonnegative function.

(A) Further assume that  $\sigma(\lambda, \mu(\lambda)) \geq 0$ . By Lemma 2, the trivial solution of (7) is stable. We will now show that there is no positive solution of (7) in this case. To the contrary, assume that  $w(\lambda, \mu(\lambda))$  is a positive solution of (7). Note that  $w(\lambda, \mu(\lambda))(x) \leq 1$ ;  $x \in \overline{\Omega}$ . Using Green's Second Identity we have:

$$\int_{\Omega} -\Delta w \phi + \Delta \phi w dx = \int_{\partial \Omega} -\frac{\partial w}{\partial \eta} \phi + \frac{\partial \phi}{\partial \eta} w ds.$$
 (19)

But, the right-hand-side of (19) is clearly equal to zero and thus:

$$0 = \int_{\Omega} -\Delta w \phi + \Delta \phi w dx = \int_{\Omega} \lambda f(w) \phi - \sigma (\lambda, \mu(\lambda)) \phi w - \lambda f'(0) \phi w$$
$$= \int_{\Omega} \left[ \lambda f(w) - \lambda f'(0) w - \sigma (\lambda, \mu(\lambda)) w \right] \phi dx$$
$$= \int_{\Omega} \left[ \lambda \left[ f(w) - f'(0) w \right] - \sigma (\lambda, \mu(\lambda)) w \right] \phi dx.$$
(20)

Now, define H(s) := f(s) - f'(0)s. By (H1), it is easy to see that H(0) = f(0) = 0 and H'(s) = f'(s) - f'(0) < 0 for s > 0 since f''(s) < 0; [0, 1]. Thus, H(s) < 0; (0, 1]. This fact combined with w > 0;  $\Omega$  and  $\sigma(\lambda, \mu(\lambda)) \ge 0$  give a contradiction. Hence, (7) has no positive solution. Since  $\psi \equiv 0$  is a solution of (7) it is also a subsolution. Next, let  $Z \equiv N$  for N > 1 giving that:

$$-\Delta Z - \lambda f(Z) > 0; \Omega$$

$$\frac{\partial Z}{\partial \eta} + \mu(\lambda)(x)Z \ge 0; \partial \Omega$$
(21)



20 Page 12 of 31 J. T. Cronin et al.

since f(Z) < 0 for Z > 1 and  $\mu(\lambda)(x) \ge 0$ ;  $x \in \partial \Omega$ . This implies that Z is a strict supersolution of (7). The lack of a positive solution combined with a global supersolution  $Z \equiv N$  for all N > 1 ensures that the trivial solution is globally asymptotically stable (see, e.g., Pao 1992).

(B) In this case, assume that  $\sigma(\lambda, \mu(\lambda)) < 0$ . By Lemma 2, the trivial solution of (7) is unstable. We will first show existence of a positive solution to (7) using the method of sub-supersolutions (see, e.g., Pao 1992). Note that since f is smooth, Taylor's Theorem ensures that given a y > 0 there is a constant  $C_y \in (0, y)$  such that:

$$f(0+y) = f(0) + f'(0)y + \frac{f''(C_y)}{2}y^2,$$
(22)

and using the fact that f(0) = 0 we have

$$\frac{f''(C_y)}{2}y^2 = f(y) - f'(0)y.$$
 (23)

We note that from (H1), there exists  $m^*$ ,  $M^* > 0$  such that  $-m^* \le f''(u) \le -M^*$ ; [0, 1]. Now, let  $\psi = m\phi$ , where  $\phi$  is the eigenfunction normalized such that  $\|\phi\|_{\infty} = 1$  which corresponds to  $\sigma(\lambda, \mu(\lambda))$  and m > 0 is to be chosen later, and consider:

$$I := -\Delta \psi - \lambda f(\psi) = m\sigma(\lambda, \mu(\lambda)) \phi + m\lambda f'(0)\phi - \lambda f(m\phi)$$

$$= m\sigma(\lambda, \mu(\lambda)) \phi - \lambda \left[ f(m\phi) - f'(0)m\phi \right]$$

$$= m\sigma(\lambda, \mu(\lambda)) \phi - \lambda \left[ \frac{f''(C_{m\phi})}{2} (m\phi)^2 \right]$$

$$= m\phi \left[ \sigma(\lambda, \mu(\lambda)) - \frac{\lambda f''(C_{m\phi})}{2} m\phi \right]; \Omega \qquad (24)$$

and

$$\frac{\partial \psi_1}{\partial \eta} + \mu(\lambda)(x)\psi = m\frac{\partial \phi}{\partial \eta} + m\mu(\lambda)(x)\phi$$

$$= -m\mu(\lambda)(x)\phi + m\mu(\lambda)(x)\phi$$

$$= 0; \partial\Omega.$$
(25)

Hence, if we choose  $m_1 := \frac{-2\sigma(\lambda,\mu(\lambda))}{\lambda m^*}$  then we have that:

$$\sigma(\lambda, \mu(\lambda)) = -\frac{\lambda m_1}{2} m^*$$
 (26)

or equivalently,

$$\sigma\left(\lambda,\mu(\lambda)\right) \le \frac{\lambda m}{2} f''\left(C_{m\phi}\right) \phi \tag{27}$$



implying that I < 0 and  $\psi = m\phi$  is a strict subsolution of (7) for all  $m < m_1$  (recall that  $\|\phi\|_{\infty} = 1$ ). We choose  $m_2 := \frac{-2\sigma(\lambda,\mu(\lambda))}{\lambda \min_{\overline{\psi}}(\phi)M^*}$  giving that:

$$\sigma(\lambda, \mu(\lambda)) = \frac{\lambda m_2}{2} (-M^*) \min_{\overline{O}} \{\phi\}$$
 (28)

or equivalently,

$$\sigma\left(\lambda,\mu(\lambda)\right) \ge \frac{\lambda m_2}{2} f''\left(C_{m_2\phi}\right) \phi \tag{29}$$

implying that  $I \ge 0$ ,  $\psi = m_2 \phi$  is a supersolution of (7), and  $\psi = m \phi$  is a strict supersolution of (7) for any  $m > m_2$ . Also, by a previous argument,  $Z \equiv N$  for any N > 1 is a strict supersolution of (7). It is easy to see that  $\psi < Z$ ;  $\overline{\Omega}$  by taking  $m \approx 0$ , thus the method of sub-supersolutions (see, e.g., Pao 1992) guarantees existence of a solution to (7),  $w(\lambda, \mu(\lambda))$ .

Next, we will show that (7) has at most one positive solution. Assume to the contrary that  $w_1$  and  $w_2$  are both positive solutions of (7). Since  $Z \equiv N$ , (N > 1) is a global supersolution, we can assume that  $w_1 < w_2 \le 1$ ;  $x \in \overline{\Omega}$ . By Green's Second Identity, we have that:

$$\int_{\Omega} -\Delta w_1 w_2 + \Delta w_2 w_1 dx = \int_{\partial \Omega} -\frac{\partial w_1}{\partial \eta} w_2 + \frac{\partial w_2}{\partial \eta} w_1 ds. \tag{30}$$

But, we also have that:

$$\int_{\partial\Omega} -\frac{\partial w_1}{\partial \eta} w_2 + \frac{\partial w_2}{\partial \eta} w_1 ds = \int_{\partial\Omega} \mu(\lambda)(x) w_1 w_2 - \mu(\lambda)(x) w_1 w_2 ds$$

$$= 0,$$
(31)

giving:

$$0 = \int_{\Omega} -\Delta w_1 w_2 + \Delta w_2 w_1 dx = \int_{\Omega} \left[ \lambda f(w_1) w_2 - \lambda f(w_2) w_1 \right]$$
$$= \int_{\Omega} \lambda w_1 w_2 \left[ \frac{f(w_1)}{w_1} - \frac{f(w_2)}{w_2} \right] dx$$
$$< 0 \tag{32}$$

since (H1) implies that  $\frac{f(s)}{s}$  is a decreasing function for  $s \in [0, 1]$  and  $w_1, w_2, \lambda$  are positive. This contradiction implies that  $w_1 \equiv w_2$  and (7) has a unique solution whenever  $\sigma(\lambda, \mu(\lambda)) < 0$ .

(i) A straightforward application of the maximum principal and the fact that f(s) < 0 for s > 1 implies that  $w(\lambda, \mu(\lambda))(x) \le 1$ ;  $x \in \overline{\Omega}$ .

(ii) Without loss of generality, assume that  $\sigma(\lambda, \mu(\lambda)) \to 0^-$  as  $\lambda \to \lambda_1^+$ . Since  $\sigma(\lambda, \mu(\lambda)) < 0$  for  $\lambda \approx \lambda_1$  and  $\lambda > \lambda_1$ , the argument above guarantees existence of a unique positive solution of (7),  $w(\lambda, \mu(\lambda))$ , which satisfies  $w(\lambda, \mu(\lambda)) \leq \frac{-2\sigma(\lambda, \mu(\lambda))}{\lambda \min_{\Omega}\{\phi\}M^*}\phi$ ;  $\overline{\Omega}$ . But, whenever  $\sigma(\lambda, \mu(\lambda)) = 0$ , comparing (8) and (9), along



20 Page 14 of 31 J. T. Cronin et al.

with uniqueness of the principal eigenvalue, will ensure that  $\lambda_1>0$  is a solution of  $\widetilde{E}_1(f'(0),\mu(\lambda))=\lambda$  (see Cronin et al. 2020) and  $\phi\equiv\overline{\phi}>0$ ;  $\overline{\Omega}$ . Thus, as  $\sigma\left(\lambda,\mu(\lambda)\right)\to0^-$  we must have  $\min_{\overline{\Omega}}\{\phi\}\to0$ . This and the fact that  $M^*>0$  implies that as  $\lambda\to\lambda_1^+$ , we have  $w(\lambda,\mu(\lambda))\leq\frac{-2\sigma(\lambda,\mu(\lambda))}{\lambda\min_{\overline{\Omega}}\{\phi\}M^*}\phi\to0^+$ ;  $\overline{\Omega}$ .

(iii) Assume that  $\sigma(\lambda, \mu(\lambda)) < 0$  for all  $\lambda > \lambda_2$ , for some  $\lambda_2 > 0$ . The above argument guarantees existence of a unique positive solution of (7) for all  $\lambda > \lambda_2$ . For  $\lambda > E_1^D$ , it is well known that

$$\begin{cases}
-\Delta w = \lambda f(w); & \Omega \\
w = 0; & \partial \Omega
\end{cases}$$
(33)

has a unique positive solution,  $\widetilde{w}$ , such that  $\widetilde{w} \to 1^-$  uniformly on all closed subsets of  $\Omega$  as  $\lambda \to \infty$  and  $\frac{\partial \widetilde{w}}{\partial \eta} < 0$ ;  $\partial \Omega$  (e.g., see Cantrell and Cosner 2003). But since  $\widetilde{w}$  satisfies the differential equation in (7) and

$$\frac{\partial \widetilde{w}}{\partial \eta} + \mu(\lambda)(x)\widetilde{w} = \frac{\partial \widetilde{w}}{\partial \eta}$$

$$< 0; \ \partial \Omega,$$
(34)

we also have that for  $\lambda > E_1^D$ ,  $\widetilde{w}$  is a strict subsolution of (7) and  $w(\lambda, \mu(\lambda)) \in [\widetilde{w}, 1]$ ;  $x \in \overline{\Omega}$ . Thus, as  $\lambda \to \infty$  we have that  $w(\lambda, \mu(\lambda)) \to 1^-$  uniformly on all closed subsets of  $\Omega$ .

(iv) Fix  $x \in \Omega$ , let  $\mu_1(\lambda)(x) \le \mu_2(\lambda)(x)$ ;  $\partial \Omega$ , and denote  $w_i(\lambda)$  as the unique positive solution of (7) with  $\mu(\lambda) \equiv \mu_i(\lambda)$ , with i = 1, 2. Now we substitute  $w_1$  into (7) with  $\mu(\lambda) \equiv \mu_2(\lambda)$  giving:

$$-\Delta w_1 - \lambda w_1 f(w_1) = 0; \ \Omega \tag{35}$$

and

$$\begin{split} \frac{\partial w_1}{\partial \eta} + \mu_2(\lambda)(x)w_1 &= -\mu_1(\lambda)(x)w_1 + \mu_2(\lambda)(x)w_1 \\ &= w_1 \left[ \mu_2(\lambda)(x) - \mu_1(\lambda)(x) \right] \\ &\geq 0; \ \partial \Omega. \end{split}$$

Thus,  $w_1$  is a supersolution of (7) with  $\mu(\lambda) \equiv \mu_2(\lambda)$  and  $Z \equiv N$ , for N > 1 is a strict supersolution of (7). Uniqueness of the positive solution of (7) guarantees that  $w_1(\lambda)(x) \geq w_2(\lambda)(x)$ ;  $x \in \overline{\Omega}$ , giving that  $w(\lambda, \mu(\lambda))$  is a decreasing function of  $\mu$ . (v) Let  $\lambda^* > \lambda^{**} > 0$  such that  $\sigma(\lambda^*, \mu(\lambda^*)), \sigma(\lambda^{**}, \mu(\lambda^{**})) < 0$  with  $\mu(\lambda^*)(x) \leq \mu(\lambda^{**})(x)$ ;  $\overline{\Omega}$ . Denote  $w_1, w_2$  as the unique positive solutions of (7) for  $\lambda^*, \lambda^{**}$ , respectively. Then,  $w_1$  satisfies:

$$-\Delta w_1 - \lambda^{**} f(w_1) \ge -\Delta w_1 - \lambda^* f(w_1) = 0; \ \Omega$$
 (36)



and

$$\frac{\partial w_1}{\partial \eta} + \mu(\lambda^{**})(x)w_1 \ge \frac{\partial w_1}{\partial \eta} + \mu(\lambda^*)(x)w_1 = 0; \ \partial\Omega. \tag{37}$$

Thus,  $w_1$  is a supersolution of (7) with  $\lambda = \lambda^{**}$ . A standard comparison principle and uniqueness of positive solutions for (7) give that  $w_1 \ge w_2$ ;  $\overline{\Omega}$ , as desired.

### 2.2 Proof of Lemma 4

Let  $\gamma_1, \gamma_2, r > 0$  and  $\beta \ge 0$  be fixed. For all  $\lambda > E_1(1, \gamma_1)$ , we have that  $\mu_2(\lambda)(x) = \sqrt{\lambda}\gamma_2 \le \sqrt{\lambda}\gamma_2$  ( $\beta u(\lambda, x) + 1$ ) =  $\mu_3(\lambda)(x)$ ;  $x \in \partial\Omega$ . Since  $\sigma(\lambda, \mu(\lambda))$  is increasing in  $\mu$  (see, e.g., Cantrell and Cosner 2003), we have that  $\sigma(\lambda, \mu_2(\lambda)) \le \sigma(\lambda, \mu_3(\lambda))$  for all  $\lambda > E_1(1, \gamma_1)$ .

Now, fix  $\mu(\lambda)(x) \ge 0$ ;  $\partial \Omega$  and note that by Green's Second Identity we have

$$\int_{\Omega} -\Delta\phi_0 \phi + \Delta\phi\phi_0 dx = \int_{\partial\Omega} -\frac{\partial\phi_0}{\partial\phi} + \frac{\partial\phi}{\partial\eta}\phi_0 ds.$$
 (38)

But, it is easy to see that

$$\int_{\Omega} -\Delta\phi_0 \phi + \Delta\phi\phi_0 dx = \int_{\Omega} (\sigma_0(\lambda) + \lambda r) \, \phi\phi_0 - (\sigma(\lambda, \mu(\lambda)) + \lambda r) \, \phi\phi_0 dx$$
$$= \int_{\Omega} (\sigma_0(\lambda) - \sigma(\lambda, \mu(\lambda))) \, \phi\phi_0 dx \tag{39}$$

and

$$\int_{\partial\Omega} -\frac{\partial\phi_0}{\partial\phi} + \frac{\partial\phi}{\partial\eta}\phi_0 ds = \int_{\partial\Omega} -\frac{\partial\phi_0}{\partial\eta}\phi ds > 0$$
 (40)

since  $\frac{\partial \phi_0}{\partial \eta} < 0$ ;  $\partial \Omega$ ,  $\phi_0 = 0$ ;  $\partial \Omega$ , and  $\phi$ ,  $\phi_0 > 0$ ;  $\Omega$ . Combining (38)–(40) yields,

$$\int_{\Omega} (\sigma_0(\lambda) - \sigma(\lambda, \mu(\lambda))) dx > 0$$
(41)

implying that  $\sigma(\lambda, \mu(\lambda)) < \sigma_0(\lambda)$  for all non-negative functions  $\mu(\lambda)$ .

### 3 Results

In this section, we provide dynamics of the model (3) over patch size for three cases: (1)  $E_1(1, \gamma_1) < E_1(r, \gamma_2)$  (i.e., predator has smaller minimum patch size), (2)  $E_1(1, \gamma_1) > E_1(r, \gamma_2)$  (i.e., prey has smaller minimum patch size), and (3)  $E_1(1, \gamma_1) = E_1(r, \gamma_2)$  (i.e., predator and prey have equal minimum patch size). We also provide a pictorial description of these results and present numerically generated



20 Page 16 of 31 J. T. Cronin et al.

density vs. average patch density plots (i.e., DAR plots) following the procedure outlined in Goddard et al. (2023). This DAR procedure assumes that population densities are near their equilibrium and employs bifurcation curves of positive steady states of the model (3) for  $\Omega=(0,1)$  for each case. In Sect. 3.1 we provide corresponding biological implications with proofs of our main results presented in Sect. 3.2. Throughout this section, we will denote  $u^*\equiv w(\lambda,\mu_1(\lambda))$  as the unique positive solution of (4) in the absence of v and  $v^*\equiv w(\lambda,\mu_2(\lambda))$  as the unique positive solution of (5) in the absence of v. We first state a theorem that describes when v and v exist.

**Theorem 6** Fix  $\gamma_1, \gamma_2 \ge 0$  and r > 0. Then the following hold.

- (1) If  $\lambda \leq E_1(1, \gamma_1)$  then  $u^* \equiv 0$  is the only nonnegative solution of (4) and is globally asymptotically stable. Moreover, if  $\lambda > E_1(1, \gamma_1)$  then the trivial solution is unstable,  $u^* \equiv w(\lambda, \mu_1(\lambda))$  is the globally asymptotically stable positive solution of (4), and if v is established in the patch and near its equilibrium,  $v^* \equiv w(\lambda, \mu_2(\lambda))$ , then  $(0, v^*)$  is unstable.
- (2) If  $\lambda \leq E_1(r, \gamma_2)$  then  $v^* \equiv 0$  is the only nonnegative solution of (5) and is globally asymptotically stable. In the absence of u, the trivial solution is unstable and  $v^* \equiv w(\lambda, \mu_2(\lambda))$  is the globally asymptotically stable positive solution of (5) for all  $\lambda > E_1(r, \gamma_2)$ .

The proof of Theorem 6 follows immediately from Theorem 3 and (12)–(15).

<u>Case 1:</u>  $E_1(1, \gamma_1) < E_1(r, \gamma_2)$  (Predator has smaller minimum patch size):

Fix  $\gamma_1, \gamma_2 > 0$ . Then for  $r < r^*$  we must have  $E_1(1, \gamma_1) < E_1(r, \gamma_2)$  (see Lemma 1) and the following result holds.

**Theorem 7** Fix  $\gamma_1, \gamma_2 > 0$ . Then for  $r < r^*$  and  $\beta > 0$  there exists a  $\lambda_1 \in \left(E_1(r, \gamma_2), \frac{E_1^D}{r}\right)$  and  $\lambda_2 \in \left[\lambda_1, \frac{E_1^D}{r}\right]$  such that:

- (1) For  $\lambda \in [E_1(r, \gamma_2), \lambda_1)$ , (5) has no positive solution, i.e.,  $(u^*, 0)$  is globally asymptotically stable.
- (2) For  $\lambda \in (\lambda_2, \infty)$ , (4)–(5) has a unique globally asymptotically stable solution, (u, v) and  $(u^*, 0)$  and  $(0, v^*)$  are unstable.

Fig. 2 gives a pictorial representation of Theorem 7 and Fig. 3 illustrates DAR via bifurcation curves of positive solutions of (4) - (5) as patch size varies for different  $\beta$ -values.

Since consumptive effects are not included in our model, Theorem 7(1) reveals that predator exclusion of prey for  $\lambda \in [E_1(r, \gamma_2), \lambda_1)$  is due solely to trait-mediated emigration. We define this phenomenon as <u>trait-mediated exclusion</u> and note that is analogous to competitive exclusion in competitive systems. Although our numerical results for the case when  $\Omega = (0, 1)$  show that  $\lambda_1 = \lambda_2$ , in a general domain we cannot rule out  $\lambda_1 < \lambda_2$  with multiple regions of coexistence and trait-mediated exclusion for  $\lambda \in (\lambda_1, \lambda_2)$ . The exact dynamics of the model in this range of  $\lambda$ -values is most likely dependent upon the geometry of  $\Omega$ .

Case 2:  $E_1(1, \gamma_1) > E_1(r, \gamma_2)$  (Prey has smaller minimum patch size):

Fix  $\gamma_1$ ,  $\gamma_2 > 0$ . Then for  $r > r^*$  we must have  $E_1(1, \gamma_1) > E_1(r, \gamma_2)$  (again, see Lemma 1) and there exist critical trait-mediated effect strength thresholds  $0 < \beta_1 < \beta_2$  such that the following results hold.



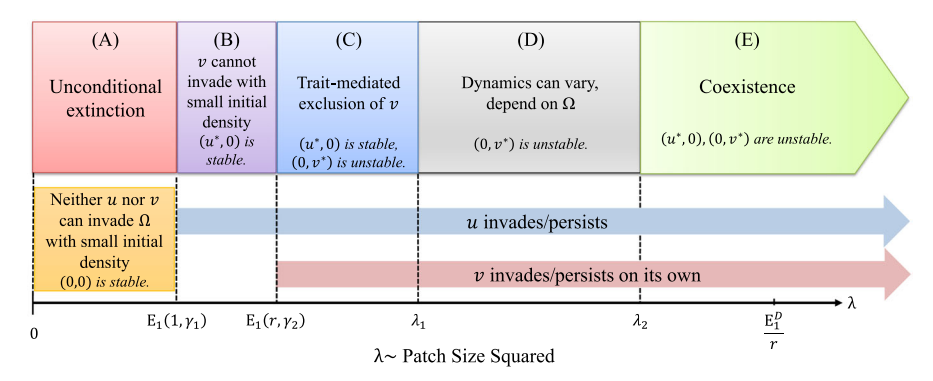


Fig. 2 Pictorial description of Theorem 7

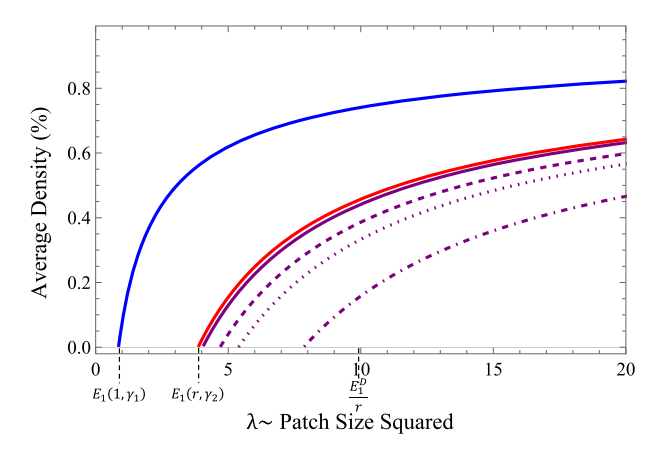


Fig. 3 Density-area relationship predicted by the model (3) for various trait-mediated effect strengths, i.e.,  $\beta$ -values. The blue curve represents both (u,0) and the u-component of the coexistence state, red represents (0,v), and purple represents the v-component of the coexistence state. Solid purple is  $\beta=0.1$ , dashed is  $\beta=0.5$ , dotted is  $\beta=1$ , and dot-dashed is  $\beta=5$ . Here,  $\gamma=1$ ,  $\gamma_1=0.5$ , and  $\gamma_2=1.5$ 

**Theorem 8** Fix  $\gamma_1$ ,  $\gamma_2 > 0$ . Then for  $r > r^*$ ,  $\beta < \beta_2$ , and  $\lambda \in (E_1(1, \gamma_1), \infty)$ , (4)–(5) has a unique globally asymptotically stable solution, (u, v), and  $(u^*, 0)$  and  $(0, v^*)$  are unstable.

Fig. 4 gives a pictorial representation of Theorem 8 and Fig. 5 illustrates DAR via a bifurcation curve of positive solutions of (4) - (5) as patch size varies for a fixed  $\beta \approx 0$ .

**Theorem 9** Fix  $\gamma_1, \gamma_2 > 0$ . Then for  $r > r^*$  and  $\beta \in (\beta_1, \beta_2)$  there exists a  $\lambda_1 \in \left(E_1(1, \gamma_1), \frac{E_1^D}{r}\right)$  such that:

- (1) For  $\lambda \in (E_1(1, \gamma_1), \infty)$ , (4)–(5) has a unique globally asymptotically stable solution, (u, v) and  $(u^*, 0)$  and  $(0, v^*)$  are unstable.
- (2) For  $\lambda \in (E_1(r, \gamma_2), \lambda_1)$ , v's DAR is at least hump-shaped, i.e., DAR is overall increasing on  $(E_1(r, \gamma_2), E_1(1, \gamma_1))$  and overall decreasing on  $(E_1(1, \gamma_1), \lambda_1)$ .



20 Page 18 of 31 J. T. Cronin et al.

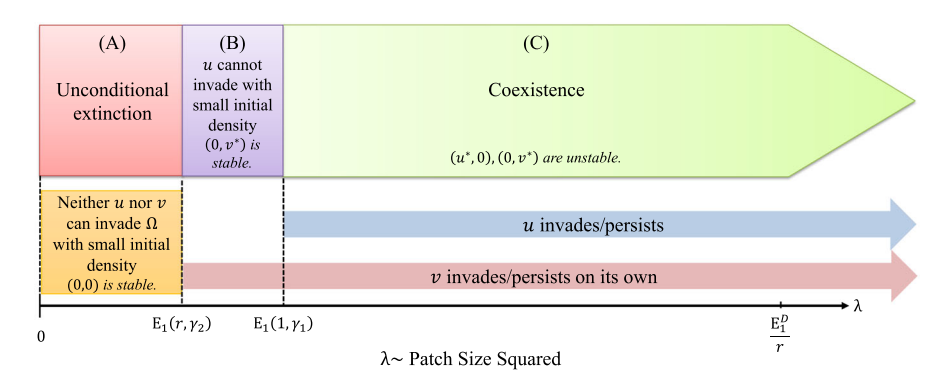
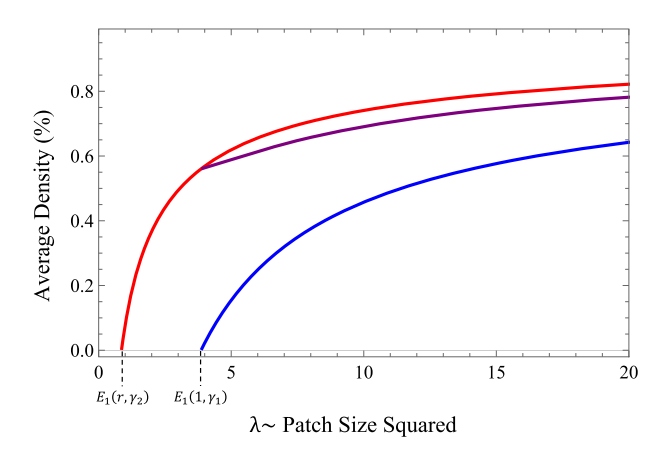


Fig. 4 Pictorial description of Theorem 8



**Fig. 5** Density-area relationship predicted by the model (3) for weak trait-mediated effect strength:  $\beta < \beta_1$ . The blue curve represents both (u,0) and the u-component of the coexistence state, red represents (0,v), and purple represents the v-component of the coexistence state. Here,  $\beta=1$ , r=1,  $\gamma_1=1.5$ , and  $\gamma_2=0.5$ 

Fig. 6 gives a pictorial representation of Theorem 9 and Fig. 7 illustrates DAR via bifurcation curves of positive solutions of (4) - (5) as patch size varies for a fixed  $\beta \in (\beta_1, \beta_2)$ .

Notice the hump-shaped DAR for v in Fig. 7.

**Theorem 10** Fix  $\gamma_1, \gamma_2 > 0$ . Then for  $r > r^*$  and  $\beta > \beta_2$  there exist  $\lambda_i$ ; i = 1, 2, 3, 4 satisfying  $E_1(1, \gamma_1) < \lambda_1 \le \lambda_2 < \lambda_3 \le \lambda_4 < \frac{E_1^D}{r}$  such that the following hold:

- (1) For  $\lambda \in (E_1(1, \gamma_1), \lambda_1)$  and  $\lambda \in (\lambda_4, \infty)$ , (4)–(5) has a unique globally asymptotically stable solution, (u, v), and  $(u^*, 0)$  and  $(0, v^*)$  are unstable.
- (2) For  $\lambda \in (\lambda_2, \lambda_3)$ , (5) has no positive solution, i.e.,  $(u^*, 0)$  is globally asymptotically stable.
- (3) For  $\lambda \in (E_1(r, \gamma_2), \lambda_1)$ , v's DAR is at least hump-shaped, i.e., DAR is overall increasing on  $(E_1(r, \gamma_2), E_1(1, \gamma_1))$  and overall decreasing on  $(E_1(1, \gamma_1), \lambda_1)$ .



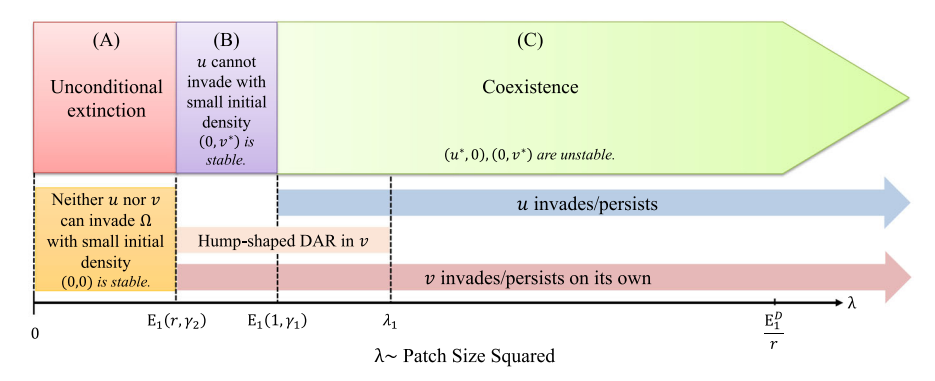


Fig. 6 Pictorial description of Theorem 9

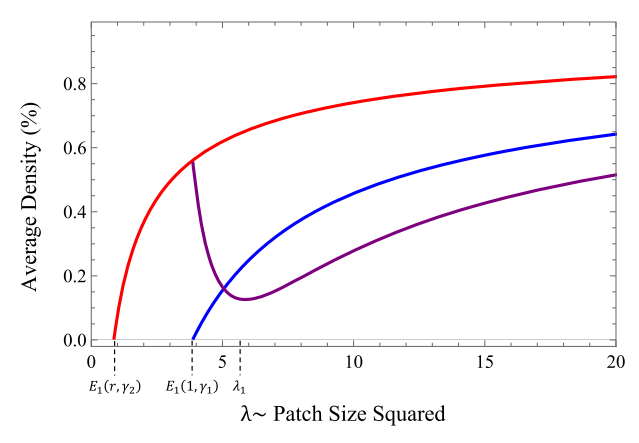


Fig. 7 Density-area relationship predicted by the model (3) for intermediate levels of trait-mediated effect strength:  $\beta \in (\beta_1, \beta_2)$ . The blue curve represents both (u, 0) and the u-component of the coexistence state, red represents (0, v), and purple represents the v-component of the coexistence state. Here,  $\beta = 20$ , r = 1,  $\gamma_1 = 1.5$ , and  $\gamma_2 = 0.5$ 

Fig. 8 gives a pictorial representation of Theorem 10 and Fig. 9 illustrates DAR via bifurcation curves of positive solutions of (4) - (5) as patch size varies for a fixed  $\beta > \beta_2$ .

Again, notice the hump-shaped DAR for v in Fig. 9. For the one-dimensional patch examples illustrated in Figs. 5, 7, and 9, we numerically estimated critical trait-mediated strength thresholds as  $\beta_1 \approx 1.75$  &  $\beta_2 \approx 29.375$  and plotted predator density-prey emigration curves (i.e., u vs.  $1 - \alpha_2(u)$ ) in Fig. 10 for the  $\beta$ 's employed. Notice that the grey shaded region in Fig. 10 represents density-emigration curves for weak trait-mediated effect strength  $\beta \in (0, \beta_1)$ , green shaded for intermediate trait-mediated effect strength  $\beta \in (\beta_1, \beta_2)$ , and red shaded for strong trait-mediated effect strength  $\beta \in (\beta_1, \beta_2)$ , and red shaded for strong trait-mediated effect strength  $\beta \in (\beta_2, \infty)$ . We note that although our numerical results for the case when  $\Omega = (0, 1)$  show that  $\lambda_1 = \lambda_2$  and  $\lambda_3 = \lambda_4$ , in a general domain we cannot rule out  $\lambda_1 < \lambda_2$  and  $\lambda_3 < \lambda_4$  with multiple regions of coexistence and trait-mediated exclusion for  $\lambda \in (\lambda_1, \lambda_2)$  and/or for  $\lambda \in (\lambda_3, \lambda_4)$ . The exact dynamics of the model in this range of  $\lambda$ -values is most likely dependent upon the geometry of  $\Omega$ .



20 Page 20 of 31 J. T. Cronin et al.

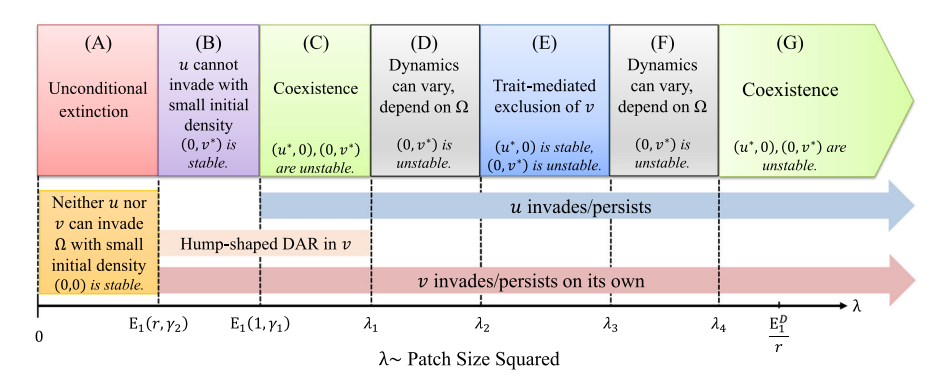
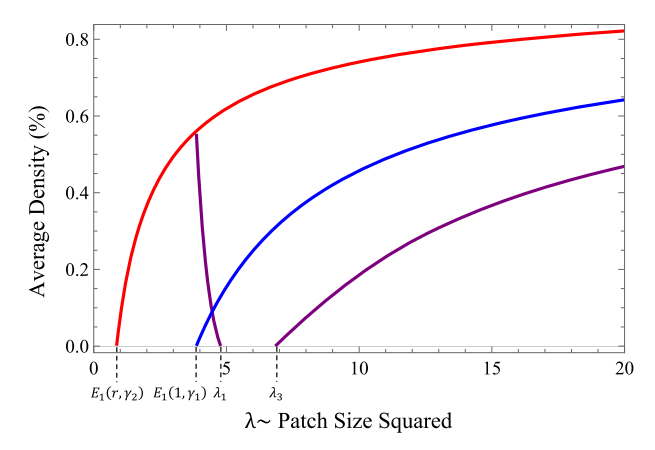


Fig. 8 Pictorial description of Theorem 10



**Fig. 9** Density-area relationship predicted by the model (3) for high levels of trait-mediated effect strength:  $\beta > \beta_2$ . The blue curve represents both (u,0) and the u-component of the coexistence state, red represents (0,v), and purple represents the v-component of the coexistence state. Here,  $\beta=35, r=1, \gamma_1=1.5, \text{ and } \gamma_2=0.5$ 

## <u>Case 3:</u> $E_1(1, \gamma_1) = E_1(r, \gamma_2)$ (Predator and prey have equal minimum patch size):

Fix  $\gamma_1, \gamma_2 > 0$ . Then for  $r = r^*$  we must have  $E_1(1, \gamma_1) = E_1(r, \gamma_2)$  (again, see Lemma 1) and the following result holds.

**Theorem 11** Fix  $\gamma_1, \gamma_2 > 0$ . Then for  $r = r^*$  we have that:

- (1) Given a  $\lambda_0 \in \left(E_1(r, \gamma_2), \frac{E_1^D}{r}\right)$ , there exists a  $\beta_1 > 0$  and  $\lambda_1, \lambda_2$  satisfying  $E_1(r, \gamma_2) \leq \lambda_1 < \lambda_0 < \lambda_2 < \frac{E_1^D}{r}$  such that (5) has no positive solution and  $(u^*, 0)$  is globally asymptotically stable for  $\lambda \in (\lambda_1, \lambda_2)$  and for  $\beta > \beta_1$ .
- (2) For all  $\beta \geq 0$ , there exists  $\lambda_3 \in \left(E_1(r, \gamma_2), \frac{E_1^D}{r}\right)$  such that for  $\lambda \in (\lambda_3, \infty)$ , (4)–(5) has a unique globally asymptotically stable solution, (u, v) and  $(u^*, 0)$  and  $(0, v^*)$  are unstable.



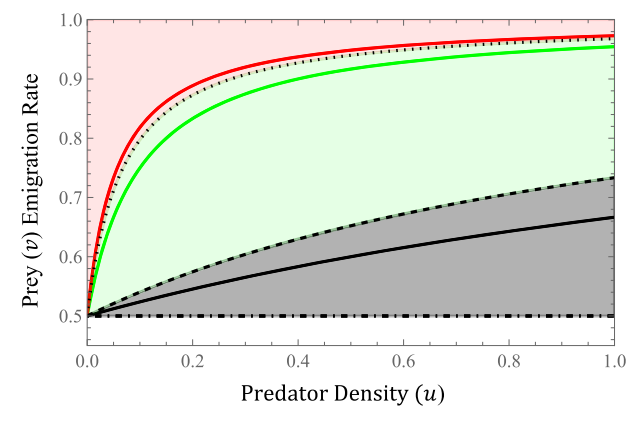


Fig. 10 Predator density-prey emigration relationships for varying trait-mediated effect strength, i.e.,  $\beta=0$  in dot-dashed black (i.e., density independent emigration),  $\beta=1$  in solid black,  $\beta=20$  in solid green, and  $\beta=35$  in solid red. The grey shaded region represents predator density-prey emigration relationships for weak trait-mediated effect strength  $\beta\in(0,\beta_1)$  with dashed black representing  $\beta=\beta_1$ , green shaded region for intermediate trait-mediated effect strength  $\beta\in(\beta_1,\beta_2)$  with dotted black representing  $\beta=\beta_2$ , and red shaded region for strong trait-mediated effect strength  $\beta\in(\beta_2,\infty)$ 

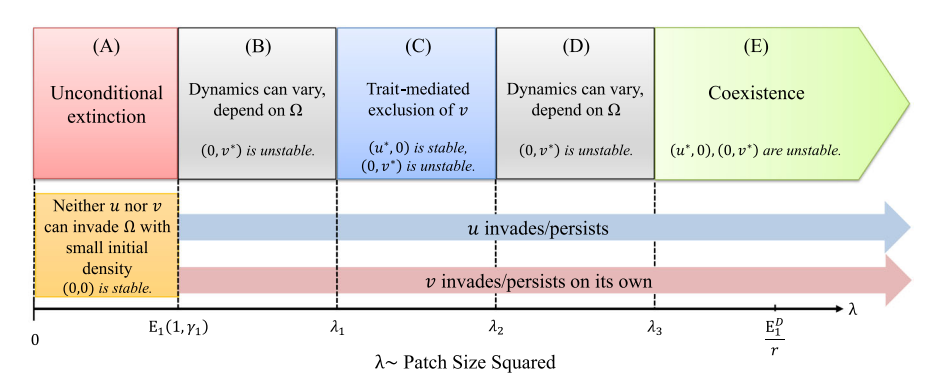


Fig. 11 Pictorial description of Theorem 11

Figure 11 gives a pictorial representation of Theorem 11 and Fig. 12 illustrates DAR via bifurcation curves of positive solutions of (4) - (5) as patch size varies for different  $\beta$ -values.

Again, we note that although our numerical results for the case when  $\Omega = (0, 1)$  show that  $\lambda_1 = E_1(1, \gamma_1)$  and  $\lambda_2 = \lambda_3$ , in a general domain we cannot rule out  $E_1(1, \gamma_1) < \lambda_1$  and  $\lambda_2 < \lambda_3$  with multiple regions of coexistence and trait-mediated exclusion for  $\lambda \in (E_1(1, \gamma_1), \lambda_1)$  and/or  $\lambda \in (\lambda_2, \lambda_3)$ . The exact dynamics of the model in this range of  $\lambda$ -values is most likely dependent upon the geometry of  $\Omega$ .

### 3.1 Biological implications

We first reiterate the fact that our model assumes direct effects (consumptive) are negligible. Certainly in a real-world predator-prey system direct effects play a cru-



20 Page 22 of 31 J. T. Cronin et al.

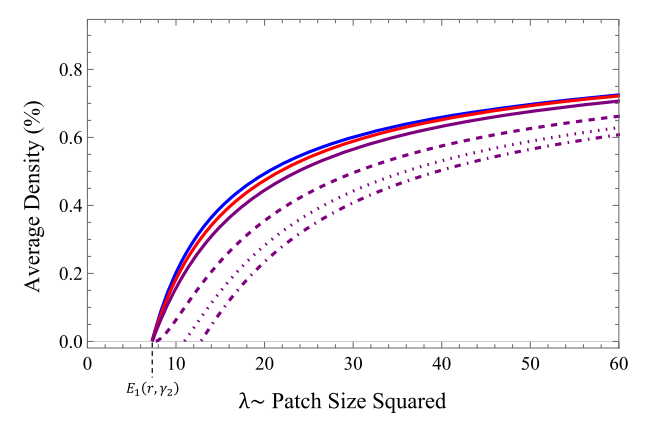


**Fig. 12** Density-area relationship predicted by the model (3) for various trait-mediated effect strengths, i.e.,  $\beta$ -values. The blue curve represents both (u, 0) and the u-component of the coexistence state, red represents (0, v), and purple represents the v-component of the coexistence state. Solid purple is  $\beta = 1$ , dashed is  $\beta = 5$ , dotted is  $\beta = 10$ , and dot-dashed is  $\beta = 15$ . Here,  $\gamma = 0.5$ ,  $\gamma_1 = 4.47662$ , and  $\gamma_2 = 1$ 

cial role in determining coexistence. However, our main goal in this current work is to disentangle direct and indirect effects and focus solely on consequences of trait-mediated emigration. In our model assumptions, the parameter  $\beta = \frac{1}{M}$  represents trait-mediated emigration effect strength in that it affects how quickly prey (v) emigration rate increases as predator density (u) increases (see Fig. 1). In other words, when  $\beta = 0$ , emigration is independent of u's density. For  $\beta \approx 0$ , presence of u has little effect on v's emigration rate, whereas for  $\beta \gg 1$ , emigration rate approaches 100% even for small densities of u.

The model predicts coexistence for patch sizes large enough such that  $\lambda > \frac{E_1^D}{r} - \delta_1(\beta)$  for some  $\delta_1(\beta) > 0$ , regardless of the trait-mediated emigration effect strength (recall that  $\lambda = E_1^D$  is the principal eigenvalue of Laplace's equation with absorbing boundary conditions and corresponds to minimum patch size for a immediately lethal matrix). In this case, sufficiently large patches develop a correspondingly large core region where the chance of an individual encountering mortality at the patch/matrix interface is very small. Exactly the opposite effect occurs for patches with  $\lambda < \min\{E_1(1, \gamma_1), E_1(r, \gamma_2)\}$  where the model predicts that neither species is able to survive in the patch. In this case, the patch is so small that a large percentage of the population enter the hostile matrix and face mortality there.

In the case that the predator has a smaller minimum patch size requirement (i.e., Case 1:  $E_1(1, \gamma_1) < E_1(r, \gamma_2)$ ), the model predicts that whenever trait-mediated emigration is present, there is a range of patch sizes with  $\lambda \in [E_1(r, \gamma_2), \lambda_1)$  (for some  $\lambda_1 = \lambda_1(\beta) > E_1(r, \gamma_2)$ ) where prey are able to colonize the patch when alone, but predicted to go extinct in the presence of the predator, i.e., trait-mediated exclusion. Since consumptive effects are not included in our model, this effect is due solely to trait-mediated emigration. Mechanistically, trait-mediated emigration causes an increase in prey emigration probability due to predator presence, which in turn, causes a larger proportion of the population to emigrate into the hostile matrix and encounter mortality there, increasing minimum patch size requirements for prey.



We also make note that (ii) from Sect. 3.2.3 holds in this case, giving that for fixed  $\lambda_0 < \frac{E_1^D}{r}$ , taking  $\beta \gg 1$  will ensure trait-mediated exclusion of prey for a range of  $\lambda$  around this  $\lambda_0$ . Thus, it is easy to see that the upper limit of the trait-mediated emigration region of  $\lambda$ ,  $\lambda_1(\beta)$ , is increasing in  $\beta$  and  $\lambda_1(\beta) \to \frac{E_1^D}{r}$  as  $\beta \to \infty$ . In other words, the length of the region of patch sizes for which trait-mediated exclusion is predicted to occur is an increasing function of trait-mediated emigration effect strength and has a maximal range which is approached as this strength goes to infinity. Thus, prey minimum patch size is a function, not only of G-D ratios (r) and combined matrix hostilities  $(\gamma_1, \gamma_2)$ , but also predator density and trait-mediated effect strength. Figure 3 illustrates the increasing nature of this trait-mediated exclusion region as the trait-mediated emigration strength is increased. We expect that patch geometry will also play a significant role in determining if there are multiple regions of coexistence and/or trait-mediated exclusion occurring for  $\lambda \in (\lambda_1, \lambda_2)$  from Theorem 7 (see Goddard et al. 2023 where this was the case in a competitive L-V model with absorbing boundary conditions). However, exploration of such effects are outside of the scope of this work.

When prey have a smaller minimum patch size requirement (i.e., Case 2:  $E_1(1, \gamma_1) > E_1(r, \gamma_2)$ , trait-mediated emigration strength plays a vital role in determining community structure. As indicated in Theorems 8 and 9, when trait-mediated emigration strength is not too strong (i.e.,  $\beta < \beta_2$ ) the model predicts coexistence for all patch sizes with  $\lambda > E_1(1, \gamma_1)$ . However, when trait-mediated emigration strength is sufficiently strong (i.e.,  $\beta > \beta_2$ ), at least one range of patch sizes emerges where trait-mediated exclusion is predicted by the model (see Theorem 10 and Figs. 8 and 9). Interestingly, for sufficiently strong trait-mediated emigration strength (i.e.,  $\beta > \beta_1$ ), the model predicts an overall hump-shaped DAR for prey for patch sizes with  $\lambda \in (E_1(r, \gamma_2), \lambda_1)$  with apex patch size corresponding to  $\lambda = E_1(1, \gamma_1)$  (see Theorems 9 and 10 and Figs. 8 and 9). The "overall" modifier is employed here since we cannot guarantee that prey DAR is strictly increasing on  $\lambda \in (E_1(r, \gamma_2), E_1(1, \gamma_1))$ and strictly decreasing on  $(E_1(r, \gamma_2), \lambda_1)$ . Also, the range of patch sizes for which a hump-shaped DAR is predicted is bound to a finite range patch sizes with corresponding  $\lambda \in \left(E_1(r, \gamma_2), \frac{E_1^D}{r}\right)$ . Mechanistically, this hump-shaped DAR arises from interaction with trait-mediated emigration and differences in minimum patch size requirements of both prey and predator. Essentially, what we coin as a dispersal release occurs at  $\lambda = E_1(1, \gamma_1)$ , which corresponds to the predator's minimum patch size. In other words, for patches with  $\lambda > E_1(1, \gamma_1)$  but  $\lambda \approx E_1(1, \gamma_1)$ , as patch size decreases an overall decrease in predator density causes a release in dispersal via reduction in emigration due to presence of predators. When trait-mediated emigration strength is sufficiently strong, positive effects on prey density via dispersal release overcome negative effects on prey density caused by a decreasing patch size, giving rise to an overall increasing DAR for decreasing patch size when  $\lambda \in (E_1(1, \gamma_1), \lambda_1)$ .

A similar hump-shaped DAR has been observed in competitive systems (which only included direct, consumptive effects) both in empirical studies (see e.g., Buckley and Roughgarden 2006) and in theoretical studies with competitive models employing absorbing boundary conditions (see Goddard et al. 2023). In those studies, a primary competitive release was predicted to occur when the competitor with a larger minimum



20 Page 24 of 31 J. T. Cronin et al.

patch size requirement lost its ability to colonize the patch when rare at its minimum patch size. With competitive release as the primary mechanism, Goddard et al. (2023) showed theoretical examples of hump-shaped DAR occurring for arbitrarily large patch sizes, as well as examples of complex geometry creating multiple hump-shaped DARs as patch size varies. We see a similar hump-shaped DAR being predicted in our model, but with a different mechanistic cause. Since this trait-mediated emigration effect is limited to patch sizes with corresponding  $\lambda < \frac{E_1^D}{r}$ , we do not expect to see hump-shaped DAR for large patch sizes (i.e., those with  $\lambda > \frac{E_1^D}{r}$ ). However, we conjecture that multiple hump-shaped DAR could be possible for patches with nonconvex geometry and patch sizes with  $\lambda < \frac{E_1^D}{r}$ , as was observed in Goddard et al. (2023).

Finally, in the case that predator and prey have equal minimum patch size requirements (i.e., Case 3:  $E_1(1,\gamma_1)=E_1(r,\gamma_2)$ ), the model predicts that whenever trait-mediated emigration is present and sufficiently strong, there is a range of patch sizes with  $\lambda \in [\lambda_1, \lambda_2)$  (for some  $E_1(r,\gamma_2) \leq \lambda_1 < \lambda_2 < \frac{E_1^D}{r}$ ) where prey are able to colonize the patch when alone, but predicted to go extinct in the presence of the predator. Also, the model predicts coexistence for patch sizes large enough such that  $\lambda > \lambda_3$  for some  $\lambda_3 \in \left[\lambda_2, \frac{E_1^D}{r}\right]$ , regardless of the trait-mediated emigration effect strength (see Theorem 11 and Figs. 11 and 12). In our one-dimensional patch example, we found that  $\lambda_1 = E_1(r,\gamma_2)$  and  $\lambda_2 = \lambda_3$ . However, in a general domain, we cannot ensure that this is always the case.

### 3.2 Proof of main results

In this section, we present proofs of our main results.

### 3.2.1 Proof of Theorem 7

Fix  $\gamma_1$ ,  $\gamma_2 > 0$ ,  $\beta > 0$ , and  $r < r^*$  implying that  $E_1(1, \gamma_1) < E_1(r, \gamma_2)$ .

- (1) By Theorem 6,  $u(E_1(r, \gamma_2))(x) > 0$ ;  $\overline{\Omega}$  and thus  $\mu_3(\lambda)(x) = \sqrt{\lambda}\gamma_2$  ( $\beta u(\lambda)(x) + 1$ ) >  $\sqrt{\lambda}\gamma_2 = \mu_2(\lambda)(x)$  for  $\lambda = E_1(r, \gamma_2)$ . Also, by (15) we have that  $\sigma(\lambda, \mu_2(\lambda)) = 0$  for  $\lambda = E_1(r, \gamma_2)$ . Thus, by Lemma 4,  $0 = \sigma(\lambda, \mu_2(\lambda)) < \sigma(\lambda, \mu_3(\lambda))$  for  $\lambda = E_1(r, \gamma_2)$ . By continuity of  $\sigma(\lambda, \mu(\lambda))$  with respect to  $\mu$  (see, e.g., Cantrell and Cosner 2003), there exists a  $\lambda_1 > E_1(r, \gamma_2)$  such that  $\sigma(\lambda, \mu_3(\lambda)) > 0$  for  $\lambda \in [E_1(r, \gamma_2), \lambda_1)$ . Theorems 3 and 6 now give that (5) has no positive solution for  $\lambda < \lambda_1$ , implying that  $(u^*, 0)$  is globally asymptotically stable.
- (2) Since  $\sigma_0(\lambda) = 0$  when  $\lambda = \frac{E_1^D}{r}$ , Lemma 4 implies that  $\sigma(\lambda, \mu_3(\lambda)) < \sigma_0(\lambda) = 0$  for  $\lambda = \frac{E_1^D}{r}$ . Again, by continuity of  $\sigma(\lambda, \mu(\lambda))$  with respect to  $\mu$ , there exists a  $\lambda_2 \in \left[\lambda_1, \frac{E_1^D}{r}\right]$  such that  $\sigma(\lambda, \mu_3(\lambda)) < 0$  for  $\lambda \in \left(\lambda_2, \frac{E_1^D}{r}\right)$ . Theorems 3 and 6 now give the result.

### 3.2.2 Proof of Theorem 8

Fix  $\gamma_1, \gamma_2 > 0$  and let  $r > r^*$ ,  $\beta > 0$ , and  $\lambda \in (E_1(1, \gamma_1), \infty)$ . By (15),  $\sigma(\lambda, \mu_2(\lambda)) < 0$  for  $\lambda > E_1(1, \gamma_1) > E_1(r, \gamma_2)$ . Now, define  $\delta := \min_{\lambda \in \left[E_1(1, \gamma_1), \frac{E_1^D}{r}\right]} \min_{x \in \overline{\Omega}} \left\{u(\lambda)(x)\right\} \geq 0$ . Thus, we have  $\mu_3(\lambda)(x) = \sqrt{\lambda}\gamma_2 \left(\beta u(\lambda)(x) + 1\right) \geq \sqrt{\lambda}\gamma_2 \left(\beta \delta + 1\right)$ . But, by choosing  $\beta \approx 0$ , we can make  $\mu_3(\lambda) \approx \sqrt{\lambda}\gamma_2 = \mu_2(\lambda)$ . By continuity of  $\sigma(\lambda, \mu(\lambda))$  with respect to  $\mu$ , we can choose  $\beta \approx 0$  such that  $\sigma(\lambda, \mu_3(\lambda)) < 0$  for  $\lambda \in \left[E_1(1, \gamma_1), \frac{E_1^D}{r}\right]$ . Also, the same argument as in (2) of the proof of Theorem 7 ensures that  $\sigma(\lambda, \mu_3(\lambda)) < 0$  for  $\lambda > \frac{E_1^D}{r}$ . Theorems 3 and 6 now give the result.

### 3.2.3 Proof of Theorems 9 and 10

Fix  $\gamma_1, \gamma_2 > 0$ . Then for  $r < r^*$  we must have  $E_1(1, \gamma_1) < E_1(r, \gamma_2)$ . First, we establish that for all  $\beta \geq 0$ ,  $\sigma(\lambda, \mu_3(\lambda)) < 0$  for  $\lambda \approx E_1(1, \gamma_1)$  and  $\lambda \approx \frac{E_1^D}{r}$ . To that end, for a fixed  $\beta \geq 0$ , Theorem 6 gives that  $u(\lambda) \equiv 0$  is the only nonnegative solution of (4) for  $\lambda \leq E_1(1, \gamma_1)$ . Thus,  $\mu_3(\lambda) \equiv \mu_2(\lambda)$  implying that  $\sigma(\lambda, \mu_3(\lambda)) = \sigma(\lambda, \mu_2(\lambda)) < 0$  for  $\lambda \in (E_1(r, \gamma_2), E_1(1, \gamma_1)]$  (see (14) for the sign of  $\sigma(\lambda, \mu_2(\lambda))$ ). Since  $\sigma(\lambda, \mu_3(\lambda)) < 0$  for  $\lambda = E_1(1, \gamma_1)$ , continuity of  $\sigma(\lambda, \mu(\lambda))$  with respect to  $\mu$  implies that there exists a  $\lambda_1 > E_1(1, \gamma_1)$  such that  $\sigma(\lambda, \mu_3(\lambda)) < 0$  for  $\lambda \in [E_1(1, \gamma_1), \lambda_1)$ . Also, the argument given in the proof of Theorem 7 (2) still holds in this case implying that there exists a  $\lambda_4 \in \left[\lambda_1, \frac{E_1^D}{r}\right]$  such that  $\sigma(\lambda, \mu_3(\lambda)) < 0$  for  $\lambda \in (\lambda_4, \infty)$ . Theorems 3 and 6 now give that (4)–(5) has a unique globally asymptotically stable positive solution, (u, v), and  $(u^*, 0)$ ,  $(0, v^*)$  are both unstable for  $\lambda \in (E_1(1, \gamma_1), \lambda_1)$  and  $\lambda \in (\lambda_4, \infty)$  which establishes (1) from Theorem 10.

Secondly, for a fixed  $\lambda \in \left(E_1(1, \gamma_1), \frac{E_1^D}{r}\right)$  we note the following:

- (i) If  $\beta = 0$  then  $\mu_3(\lambda) = \mu_2(\lambda)$  implying that  $\sigma(\lambda, \mu_3(\lambda)) = \sigma(\lambda, \mu_2(\lambda)) < 0$  by (14) and since  $\lambda > E_1(1, \gamma_1) > E_1(r, \gamma_2)$ . Continuity of  $\sigma(\lambda, \mu(\lambda))$  with respect to  $\mu$  again implies that  $\sigma(\lambda, \mu_3(\lambda)) < 0$  for this fixed  $\lambda$  and  $\beta \approx 0$ .
- (ii) Since  $\lambda > E_1(1, \gamma_1)$ , Theorem 3 and (12) implies that  $u(\lambda)(x) > 0$ ;  $\overline{\Omega}$ . Comparing (9) with (8) we have that:

$$\widetilde{E}_1\left(\sigma(\lambda,\mu(\lambda)) + \lambda r, \sqrt{\lambda}\gamma_2\left(\beta u(\lambda) + 1\right)\right) = 1. \tag{42}$$

If  $\sigma(\lambda, \mu_3(\lambda)) = 0$  then (42) becomes

$$\widetilde{E}_1\left(\lambda r, \sqrt{\lambda}\gamma_2\left(\beta u(\lambda) + 1\right)\right) = 1,$$
(43)



20 Page 26 of 31 J. T. Cronin et al.

where employing (10) gives an equivalent form

$$\frac{\widetilde{E}_1\left(1, \frac{1}{\sqrt{r}}\gamma_2(\beta u(\lambda) + 1)\right)}{r} = \lambda. \tag{44}$$

Since  $\widetilde{E}_1(R, b)$  is decreasing with respect to R, if

$$\frac{\widetilde{E}_1\left(1, \frac{1}{\sqrt{r}}\gamma_2(\beta u(\lambda) + 1)\right)}{r} < \lambda \tag{45}$$

then we must have that  $\sigma(\lambda, \mu_3(\lambda)) < 0$  in order for (42) to hold. Similarly, if

$$\frac{\widetilde{E}_1\left(1, \frac{1}{\sqrt{r}}\gamma_2(\beta u(\lambda) + 1)\right)}{r} > \lambda \tag{46}$$

then we must have that  $\sigma(\lambda, \mu_3(\lambda)) > 0$ . Recall that  $\widetilde{E}_1(R, b)$  is strictly increasing in b and approaches  $\frac{E_1^D}{R}$  as  $\min_{x \in \overline{\Omega}} \{b(x)\} \to \infty$ . Thus, since  $\lambda < \frac{E_1^D}{r}$  there exists a  $\beta^* = \beta^*(\lambda) > 0$  such that  $\sigma(\lambda, \mu_3(\lambda)) > 0$  for this  $\lambda$  (in fact, for a small neighborhood around  $\lambda$ ) and for  $\beta > \beta^*(\lambda)$ . We also note that for  $\lambda > \frac{E_1^D}{r}$ , (45) implies that  $\sigma(\lambda, \mu_3(\lambda)) < 0$  for all  $\beta \geq 0$ .

Third, it is easy to see that  $\mu_3(\lambda)(x) = \sqrt{\lambda}\gamma_2 \left(\beta u(\lambda)(x) + 1\right)$  is strictly increasing in  $\beta$  for  $\lambda > E_1(1, \gamma_1)$ . By (i),  $\sigma(\lambda, \mu_3(\lambda)) < 0$  for  $\beta \approx 0$  and by (ii)  $\sigma(\lambda, \mu_3(\lambda)) > 0$  for  $\beta \gg 1$  for every fixed  $\lambda \in \left(E_1(1, \gamma_1), \frac{E_1^D}{r}\right)$ , hence there must exist a  $\beta_2 > 0$  such that:

- (a) if  $\beta < \beta_2$  then  $\sigma(\lambda, \mu_3(\lambda)) < 0$  for all  $\lambda > E_1(r, \gamma_2)$ ;
- (b) if  $\beta = \beta_2$  then there exist  $\lambda_0^i \in \left(E_1(1, \gamma_1), \frac{E_1^D}{r}\right)$  with  $i = 1, 2, ..., n \ (n \in \mathbb{N})$  such that  $\sigma(\lambda, \mu_3(\lambda)) = 0$  for  $\lambda = \lambda_0^i$  and  $\sigma(\lambda, \mu_3(\lambda)) < 0$  for  $\lambda > E_1(1, \gamma_1)$  and  $\lambda \neq \lambda_0^i$ ;
- (c) if  $\beta > \beta_2$  then there exist  $\lambda_2, \lambda_3 \in \left(E_1(1, \gamma_1), \frac{E_1^D}{r}\right)$  with  $\lambda_1 \leq \lambda_2$  and  $\lambda_3 \leq \lambda_4$  such that  $\sigma(\lambda, \mu_3(\lambda)) > 0$  for  $\lambda \in (\lambda_2, \lambda_3)$ .

Theorems 3 and 6 combined with (a) establishes (1) from Theorem 9 and combined with (c) establishes (2) from Theorem 10.

It only remains to show that DAR for v is overall hump-shaped on  $(E_1(r, \gamma_2), \lambda_1)$ . For  $\beta \geq \beta_2$ , without loss of generality, we can assume that  $\lambda_2, \lambda_3$  are the smallest such  $\lambda$ 's that satisfy  $\sigma(\lambda, \mu_3(\lambda)) > 0$  for  $\lambda \in (\lambda_2, \lambda_3)$  in (c) and  $\sigma(\lambda, \mu_3(\lambda)) = 0$  for  $\lambda = \lambda_1$  (such a choice is possible since  $\sigma(\lambda, \mu_3(\lambda)) < 0$  for  $\lambda \in (E_1(r, \gamma_2), \lambda_1)$  and  $\sigma(\lambda, \mu_3(\lambda)) > 0$  for  $\lambda \in (\lambda_2, \lambda_3)$ ). By Theorem 3, the unique positive solution of (5) satisfies  $\|v(\lambda)\|_{\infty} \to 0^+$  as  $\lambda \to \lambda_1^-$  and  $v(\lambda)(x) \equiv 0$  is the only nonnegative solution of (5) for  $\lambda \in (\lambda_2, \lambda_3)$ . Also,  $\|v(\lambda)\|_{\infty} \to 0^+$  as  $\lambda \to E_1(r, \gamma_2)^+$ . The fact that  $v(\lambda, x) > 0$ ;  $\overline{\Omega}$  for  $\lambda \in (E_1(r, \gamma_2), \lambda_1)$  and  $v(\lambda, x)$  is a decreasing



function of  $\mu_3$  immediately establishes an overall hump-shaped DAR for v since we have  $v(\lambda)(x)$  is overall increasing on  $(E_1(r, \gamma_2), E_1(1, \gamma_1))$  and overall decreasing on  $(E_1(1, \gamma_1)), \lambda_1)$ . The modifier "overall" is purposely employed here since proving that  $v(\lambda, x)$  is monotone in  $\lambda$  remains an open problem. This establishes (3) from Theorem 10.

Finally, for  $\beta = \beta_2$ , the previous argument shows that DAR for v is overall hump-shaped on  $(E_1(r, \gamma_2), \lambda_1)$ . But, Theorems 3 and 6 give that  $u(\lambda) \equiv 0$  and  $v(\lambda) > 0$ ;  $\overline{\Omega}$  for  $\lambda = E_1(1, \gamma_1)$ . Define  $\delta := \min_{x \in \overline{\Omega}} \{v(E_1(1, \gamma_1))(x)\} > 0$ . Notice that  $\delta$  is independent of  $\beta$  since  $u(\lambda)(x) \equiv 0$  for  $\lambda = E_1(1, \gamma_1)$ . By continuity of  $v(\lambda, x)$  with respect to  $\beta$ , there exists a  $\beta_1 \in (0, \beta_2)$  such that  $v(\lambda_1, x) < \delta$ ;  $\overline{\Omega}$  for  $\beta \in (\beta_1, \beta_2)$  and ensuring that v's DAR is overall decreasing on  $(E_1(1, \gamma_1), \lambda_1)$ . This establishes (2) from Theorem 9 and completes the proof.

### 3.2.4 Proof of Theorem 11

Fix  $\gamma_1, \gamma_2 > 0$ . Then for  $r = r^*$  we have that  $E_1(1, \gamma_1) = E_1(r, \gamma_2)$ . For a fixed  $\lambda_0 \in \left(E_1(r, \gamma_2), \frac{E_1^D}{r}\right)$ , (ii) from the proof of Theorem 10 establishes (1). Also, (2) immediately follows from the proof of Theorem 7 (2).

### 4 Summary and conclusion

In this paper, we have employed a model built upon the reaction diffusion framework to demonstrate that trait-mediated emigration and matrix hostility in a predator-prey system can have profound effects on DAR, minimum patch size and species coexistence, ultimately causing an overall hump-shaped DAR to arise in prey. The model includes a boundary condition designed to model effects of differential matrix hostility and behaviorial response to habitat edges between predator and prey, and to model trait-mediated emigration in prey. In order to disentangle direct (consumptive) and indirect (trait-mediated) effects on community structure, we made an assumption that the generalist predator's consumptive effect on prey is negligible. Thus, we do not expect our model to exactly match that of any particular real-world predator-prey system. However, empirical studies have used an analogous approach to partition densityfrom trait-mediated effects; for example, Oswald (1998) glued the mouthparts of spiders together to prevent them from consuming prey while allowing them to affect prey dispersal. Our main goal here is to show the varied consequences of trait-mediated emigration on system dynamics. Our results are based on study of certain eigenvalue problems and sub-supersolutions in the general patch case and time map analysis in the one-dimensional patch case.

Our analysis covered three cases in which prey had larger, smaller, or equal minimum patch size requirements as the predator based upon permeability and hostility of the matrix. In the case that the predator has a smaller minimum patch size requirement, we showed there exists a range of patch sizes for which trait-mediated exclusion of prey occurs for any trait-mediated strength. In this case, as trait-mediated effect strength increased, prey minimum patch size increased. However, when prey has a smaller



minimum patch size requirement, trait-mediated effect strength was required to be sufficiently large to ensure trait-mediated exclusion of the prey occurred. The model also predicted an overall hump-shaped prey DAR for sufficiently strong trait-mediated effect strength, due to a dispersal release occurring around the predator's minimum patch size. Using computationally generated DAR curves in the one-dimensional patch case, we explored qualitative behavior necessary to ensure such a hump-shaped DAR occurs. Our results indicated that predator density-prey emigration rate relationship needs to increase quite quickly towards 100% emigration as predator density increases even for small predator density in order to ensure a hump-shaped prey DAR occurred. Such a prediction is similar to one observed in a diffusive Lotka-Volterra competition model with absorbing boundary conditions in Goddard et al. (2023), though with a different mechanism behind the hump-shaped DAR. We have thus identified two different mechanisms capable of producing theoretical predictions of nonlinear DARs.

Trait-mediated predator effects leading to changes in DAR shape have rarely been investigated empirically. One exception is the study by Buckley and Roughgarden (2006) who suggested that avian predators may be responsible for the nonlinear DAR observed for Anolis lizards. Our study lends more credence to the possibility that predators can alter prey DAR through predator-induced prey dispersal. Given the plethora of empirical studies that have reported strong trait-mediated predator effects, sometimes even stronger than density-mediated effects (Sih et al. 1992; Hakkarainen et al. 2001; Peckarsky 1996; Cronin et al. 2004), it is likely that these indirect effects play an important role in shaping DARs in nature. This is an important knowledge gap, particularly in the area of conservation biology. Not only is DAR a key consideration in the single large or several-small (SLOSS) debate for reserve design (Simberloff and Abele 1982; Matter 1999; Bowers and Matter 1997; Heilman et al. 2002; Lindenmayer et al. 2015; Mccarthy et al. 2005), but also it is critical for understanding the minimum patch size that can support a viable population (Bender et al. 1998; McCoy and Mushinsky 2007). DARs can also be relevant to integrative pest management programs where native populations of beneficial natural enemies can be promoted by protecting or creating appropriately sized native habitats adjacent to agricultural lands (Landis et al. 2000; Jonsson et al. 2008).

A natural extension of our model is to include direct (consumptive) effects. We are currently pursing such a model in a forthcoming manuscript. Another extension of these results would be a numerical exploration of prey DAR in nonconvex domains such as the one studied in Goddard et al. (2023) to see if multiple hump-shaped DARs occur by varying patch size. We also note that trait-mediated emigration as modeled in the prey species here ultimately produces a single species model with a nonlinear emigration function of patch size via the composite parameter,  $\lambda$ . Thus, a single species whose growth satisfies our general logistic-type growth hypotheses that exhibits a nonlinear patch size-emigration rate relationship can also be studied using our framework.

**Acknowledgements** This material is based upon work supported by the National Science Foundation under Grant Nos. DMS-1853359, DMS-1853372, DMS-1853352, DMS-2150945, DMS-2150946, & DMS-2150947.



**Author Contributions** All authors contributed to the study conception and design, analysis, and writing/revising of the manuscript. If any of the sections are not relevant to your manuscript, please include the heading and write 'Not applicable' for that section.

Availability of data and materials Not applicable.

### **Declarations**

**Conflict of interest** The authors have no competing interests to declare that are relevant to the content of this article.

### References

- Acharya A, Bandyopadhyay S, Cronin JT, Goddard J, Muthunayake A, Shivaji R (2023) The diffusive Lotka–Volterra competition model in fragmented patches i: Coexistence. Nonlinear Anal Real World Appl 70:103775. https://doi.org/10.1016/j.nonrwa.2022.103775
- Amann H (1976) Nonlinear elliptic equations with nonlinear boundary conditions. North-Holland, Amsterdam, , vol 21, pp 43–63. https://doi.org/10.1016/S0304-0208(08)71154-X
- Bender DJ, Contreras TA, Fahrig L (1998) Habitat loss and population decline: a meta-analysis of the patch size effect. Ecology 79(2):517–533. https://doi.org/10.1890/0012-9658(1998)079[0517:HLAPDA]2. 0.CO:2
- Bowers MA, Matter SF (1997) Landscape ecology of mammals: relationships between density and patch size. J Mammal 78(4):999–1013. https://doi.org/10.2307/1383044
- Buckley LB, Roughgarden J (2006) A hump-shaped density-area relationship for island lizards. Oikos 113(2):243–250. https://doi.org/10.1111/j.2006.0030-1299.14401.x
- Cantrell RS, Cosner C (2003) Spatial ecology via reaction-diffusion equations. Mathematical and Computational Biology. Wiley, Chichester, p 411
- $Cantrell\,RS,\,Cosner\,C\,(2006)\,On\,the\,effects\,of\,nonlinear\,boundary\,conditions\,in\,diffusive\,logistic\,equations\,on\,bounded\,domains.\,J\,Differ\,Equ\,231:768-804$
- Cantrell RS, Cosner C (2007) Density dependent behavior at habitat boundaries and the Allee effect. Bull Math Biol 69:2339–2360. https://doi.org/10.1007/s11538-007-9222-0
- Cantrell RS, Cosner C (2018) Effects of harvesting mediated by dispersal traits. Nat Resour Model 31(4):12168. https://doi.org/10.1111/nrm.12168
- Cantrell RS, Cosner C, Fagan WF (1998) Competitive reversals inside ecological reserves: the role of external habitat degradation. J Math Biol 37(6):491–533. https://doi.org/10.1007/s002850050139
- Cantrell R, Cosner C, Lou Y (2004) Multiple reversals of competitive dominance in ecological reserves via external habitat degradation. J Dyn Differ Equ 16(4):973–1010. https://doi.org/10.1007/s10884-004-7831-y
- Connor EF, Courtney AC, Yoder JM (2000) Individuals-area relationships: the relationship between animal population density and area. Ecology 81(3):734–748. https://doi.org/10.1890/0012-9658(2000)081[0734:IARTRB]2.0.CO;2
- Cronin JT (2007) Shared parasitoids in a metacommunity: indirect interactions inhibit herbivore membership in local communities. Ecology 88(12):2977–2990. https://doi.org/10.1890/07-0253.1
- Cronin JT, Haynes KJ, Dillemuth F (2004) Spider effects on planthopper mortality, dispersal, and spatial population dynamics. Ecology 85(8):2134–2143. https://doi.org/10.1890/03-0591
- Cronin JT, Goddard J II, Shivaji R (2019) Effects of patch matrix-composition and individual movement response on population persistence at the patch-level. Bull Math Biol 81(10):3933–3975. https://doi.org/10.1007/s11538-019-00634-9
- Cronin JT, Fonseka N, Goddard J II, Leonard J, Shivaji R (2019) Modeling the effects of density dependent emigration, weak Allee effects, and matrix hostility on patch-level population persistence. Math Biosci Eng 17(2):1718–1742
- Cronin JT, Goddard J II, Muthunayake A, Shivaji R (2020) Modeling the effects of trait-mediated dispersal on coexistence of mutualists. Math Biosci Eng 17(6):7838–7861. https://doi.org/10.3934/mbe.2020399



Debinski DM, Holt RD (2000) A survey and overview of habitat fragmentation experiments. Conserv Biol 14(2):342–355. https://doi.org/10.1046/j.1523-1739.2000.98081.x

- Ewers RM, Didham RK, Pearse WD, Lefebvre V, Rosa IMD, Carreiras JMB, Lucas RM, Reuman DC (2013) Using landscape history to predict biodiversity patterns in fragmented landscapes. Ecol Lett 16(10):1221–1233. https://doi.org/10.1111/ele.12160
- Fonseka N, Goddard J II, Morris Q, Shivaji R, Son B (2020a) On the effects of the exterior matrix hostility and a u-shaped density dependent dispersal on a diffusive logistic growth model. Topol Methods Nonlinear Anal 13(12):1–15
- Fonseka N, Goddard J II, Shivaji R, Son B (2020b) A diffusive weak allee effect model with u-shaped emigration and matrix hostility. Discrete Contin Dyn Syst Ser B 26(10):5509–5517. https://doi.org/10.3934/dcdsb.2020356
- Goddard II J, Shivaji R (2017) Stability analysis for positive solutions for classes of semilinear elliptic boundary-value problems with nonlinear boundary conditions. Proc R Soc Edinb 147(A):1019–1040
- Goddard J II, Morris Q, Robinson S, Shivaji R (2018) An exact bifurcation diagram for a reaction diffusion equation arising in population dynamics. Boundary Value Problems 170:1–17. https://doi.org/10.1186/s13661-018-1090-z
- Goddard J II, Morris Q, Payne C, Shivaji R (2019) A diffusive logistic equation with u-shaped density dependent dispersal on the boundary. Topol Methods Nonlinear Anal 53(1):335–349
- Goddard J II, Shivaji R, Cronin JT (2023) Ecological release and patch geometry can cause nonlinear density-area relationships. J Theor Biol 557(21):1-14
- Hakkarainen H, Ilmonen P, Koivunen V, Korpimäki E (2001) Experimental increase of predation risk induces breeding dispersal of Tengmalm's owl. Oecologia 126(3):355–359. https://doi.org/10.1007/ s004420000525
- Hambäck PA, Englund G (2005) Patch area, population density and the scaling of migration rates: the resource concentration hypothesis revisited. Ecol Lett 8(10):1057–1065. https://doi.org/10.1111/j. 1461-0248.2005.00811.x
- Hanski I (1999) Metapopulation ecology. Oxford University Press
- Harman R, Goddard J II, Shivaji R, Cronin JT (2020) Frequency of occurrence and population-dynamic consequences of different forms of density-dependent emigration. Am Nat 195(5):851–867
- Haynes KJ, Cronin JT (2003) Matrix composition affects the spatial ecology of a prairie planthopper. Ecology 84(11):2856–2866. https://doi.org/10.1890/02-0611
- Heilman GE, Strittholt JR, Slosser NC, Dellasala DA (2002) Forest fragmentation of the conterminous United States: assessing forest intactness through road density and spatial characteristics: Forest fragmentation can be measured and monitored in a powerful new way by combining remote sensing, geographic information systems, and analytical software. Bioscience 52(5):411–422. https://doi.org/ 10.1641/0006-3568(2002)052[0411:FFOTCU]2.0.CO;2
- Holt RD, Barfield M (2012) Trait-mediated effects, density dependence and the dynamic stability of ecological systems. Cambridge University Press, Cambridge, New York
- Irwin RE (2012) The role of trait-mediated indirect interactions for multispecies plant-animal mutualisms. Cambridge University Press, Cambridge, New York, pp 257–277
- Jackson HB, Zeccarias A, Cronin JT (2013) Mechanisms driving the density-area relationship in a saproxylic beetle. Oecologia 173(4):1237–1247. https://doi.org/10.1007/s00442-013-2697-5
- Jonsson M, Wratten SD, Landis DA, Gurr GM (2008) Recent advances in conservation biological control of arthropods by arthropods. Biol Control 45(2):172–175. https://doi.org/10.1016/j.biocontrol.2008. 01.006
- Landis DA, Wratten SD, Gurr GM (2000) Habitat management to conserve natural enemies of arthropod pests in agriculture. Annu Rev Entomol 45(1):175–201. https://doi.org/10.1146/annurev.ento.45.1. 175
- Laundré JW, Hernández L, Medina PL, Campanella A, López-Portillo J, González-Romero A, Grajales-Tam KM, Burke AM, Gronemeyer P, Browning DM (2014) The landscape of fear: the missing link to understand top-down and bottom-up controls of prey abundance? Ecology 95(5):1141–1152. https://doi.org/10.1890/13-1083.1
- Laundré JW, Hernández L, Altendorf KB (2001) Wolves, elk, and bison: reestablishing the "landscape of fear" in Yellowstone National Park, USA. Can J Zool 79(8):1401–1409. https://doi.org/10.1139/z01-094



- Lindenmayer DB, Wood J, McBurney L, Blair D, Banks SC (2015) Single large versus several small: the Sloss debate in the context of bird responses to a variable retention logging experiment. For Ecol Manage 339:1–10. https://doi.org/10.1016/j.foreco.2014.11.027
- MacArthur RH (1972) Geographical ecology: patterns in the distribution of species. Princeton University Press
- Maciel GA, Lutscher F, Associate Editor: Sean HR, Editor: Troy D (2013) How individual movement response to habitat edges affects population persistence and spatial spread. Am Naturalist 182(1):42– 52. https://doi.org/10.1086/670661
- Matassa CM, Trussell GC (2011) Landscape of fear influences the relative importance of consumptive and nonconsumptive predator effects. Ecology 92(12):2258–2266. https://doi.org/10.1890/11-0424.1
- Matter SF (1999) Population density and area: the role of within- and between-generation processes over time. Ecol Model 118(2):261–275. https://doi.org/10.1016/S0304-3800(99)00051-4
- Matter SF (2000) The importance of the relationship between population density and habitat area. Oikos 89(3):613–619
- Mccarthy MA, Thompson CJ, Possingham HP (2005) Theory for designing nature reserves for single species. Am Nat 165(2):250–257
- McCoy ED, Mushinsky HR (2007) Estimates of minimum patch size depend on the method of estimation and the condition of the habitat. Ecology 88(6):1401–1407. https://doi.org/10.1890/06-1188
- Ohgushi T, Schmitz O, Holt RD (2012) Trait-mediated indirect interactions: ecological and evolutionary perspectives. Cambridge University Press, New York
- Oswald J (1998) Schmitz: Direct and indirect effects of predation and predation risk in old-field interaction webs. Am Nat 151(4):327–342. https://doi.org/10.1086/286122
- Ovaskainen O (2004) Habitat-specific movement parameters estimated using mark-recapture data and a diffusion model. Ecology 85(1):242–257. https://doi.org/10.1890/02-0706
- Ovaskainen O, Cornell SJ (2003) Biased movement at a boundary and conditional occupancy times for diffusion processes. J Appl Probab 40(3):557–580. https://doi.org/10.2307/3215936
- Pao CV (1992) Nonlinear parabolic and elliptic equations. Plenum Press, New York, p 777
- Peckarsky BL (1996) Alternative predator avoidance syndromes of stream-dwelling mayfly larvae. Ecology 77(6):1888–1905. https://doi.org/10.2307/2265793
- Sand H, Jamieson M, Andrén H, Wikenros C, Cromsigt J, Månsson J (2021) Behavioral effects of wolf presence on moose habitat selection: testing the landscape of fear hypothesis in an anthropogenic landscape. Oecologia 197(1):101–116. https://doi.org/10.1007/s00442-021-04984-x
- Schmitz OJ (2003) Top predator control of plant biodiversity and productivity in an old-field ecosystem. Ecol Lett 6(2):156–163. https://doi.org/10.1046/j.1461-0248.2003.00412.x
- Sih A, Kats LB, Moore RD (1992) Effects of predatory sunfish on the density, drift, and refuge use of stream salamander larvae. Ecology 73(4):1418–1430. https://doi.org/10.2307/1940687
- Simberloff D, Abele LG (1982) Refuge design and island biogeographic theory: effects of fragmentation. Am Nat 120(1):41–50. https://doi.org/10.1086/283968
- Uchida K, Ushimaru A (2014) Biodiversity declines due to abandonment and intensification of agricultural lands: patterns and mechanisms. Ecol Monogr 84(4):637–658. https://doi.org/10.1890/13-2170.1
- Werner EE, Peacor SD (2003) A review of trait-mediated indirect interactions in ecological communities. Ecology 84(5):1083–1100. https://doi.org/10.1890/0012-9658(2003)084[1083:arotii]2.0.co;2
- Wright SJ (1981) Extinction-mediated competition: the Anolis lizards and insectivorous birds of the West Indies. Am Nat 117(2):181–192. https://doi.org/10.1086/283697
- Wright SJ, Kimsey R, Campbell CJ (1984) Mortality rates of insular Anolis lizards: A systematic effect of island area? Am Nat 123(1):134–142. https://doi.org/10.1086/284192

**Publisher's Note** Springer Nature remains neutral with regard to jurisdictional claims in published maps and institutional affiliations.

Springer Nature or its licensor (e.g. a society or other partner) holds exclusive rights to this article under a publishing agreement with the author(s) or other rightsholder(s); author self-archiving of the accepted manuscript version of this article is solely governed by the terms of such publishing agreement and applicable law.

